MOLECULAR STRUCTURE AND SPECTROSCOPY OF MINOR CHEMICAL COMPOUNDS IN THE ATMOSPHERES OF JUPITER AND VENUS

by

IRA ROBERT PINES

A. B. (Cornell University, 1969)

A thesis submitted in partial fulfillment
of the requirements for the degree of
Master of Science

Massachusetts Institute of Technology
Cambridge, Massachusetts

August, 1971

Signature of author . . . . . .
Department of Earth and Planetary Sciences

Certified by . . . . . .
Thesis Supervisor

Accepted by . . . . . .
Chairman, Departmental Committee on
Graduate Students
Lindgren

MOLECULAR STRUCTURE AND SPECTROSCOPY OF MINOR CHEMICAL COMPOUNDS IN THE ATMOSPHERES OF JUPITER AND VENUS

by

IRA ROBERT PINES

A thesis submitted to the Department of Earth and Planetary Sciences, August, 1971 in partial fulfillment of the requirements for the degree of Master of Science.

Abstract

Studies of the molecular structure and spectroscopy of various minor chemical constituents in the atmospheres of Jupiter and Venus. Molecular orbital calculations have been carried out upon CO_3 and ClOO using the INDO/CNDO method in an attempt to investigate their chemical stability as intermediates in the photolysis of CO_2 and photodissociation of HCl respectively. The molecular structure and spectroscopy of sulfur chains S_N, N = 2, 3 . . . 8, has been investigated by means of U. V. and visible absorption spectroscopy and CNDO molecular orbital calculations. A new method of the preparation of ammonium polysulfides based upon the complexing power of large cations has been presented and also ESR spectra has been recorded demonstrating that ammonium polysulfide in various solvents is a free radical. The various red to brown colorations of Jupiter are attributed to a photolysis of H_2S producing polysulfide like compounds. Finally an INDO molecular orbital calculation has been presented for $NH_2NH_2^+$ which proves to be planar in its most stable configuration and is an intermediate between the planar ethylene and the non-planar hydrazine molecule.

Thesis supervisor: John Simpson Lewis, Ph. D.
Title: Assistant Professor of Chemistry and Geochemistry.

To My Parents, Ellen, Joyce and Arlene

Acknowledgements

I would like to warmly acknowledge the guidance and helpful discussions provided by Dr. John S. Lewis, without whose patience this thesis would have been impossible to complete. Discussions and advice of Dr. R. G. Prinn on both the subjects of molecular orbital theory and planetary atmospheres are warmly acknowledged. Also I would like to express my appreciation for the help of J. Simms, without which the experimental work would have been much more difficult. Finally I would like to thank the staff of the M. I. T. Computing Center.

Contents

1. Introduction 6

2. Molecular structure and photolysis of CO_3 8

3. Molecular structure of free radicals in the Venusian atmosphere 11

4. Spectroscopy and molecular structure of polysulfides in the Jovian atmosphere 13

5. Molecular structure of $NH_2NH_2^+$ 16

6. Conclusions 18

References 20

Appendices . . . . . .

I. LCAO-SCF-INDO calculations on the CO_3 molecule . . . . . .

II. LCAO-SCF-INDO/CNDO calculations on FOO, CLOO, F_2O_2, Cl_2O_2 and $FClO_2$ . . . . . .

III. Preparation and spectra of ammonium polysulfides . . . . . .

IV. LCAO-SCF-CNDO calculations on sulfur chains . . . . . .

V. LCAO-SCF-INDO calculations on $NH_2NH_2^+$ . . . . . .

1. Introduction

Recent advances in observational techniques used in planetary astronomy have opened the possibility of determining in part the chemical basis of various planetary atmospheres beyond the most abundant gases. In combination with the plethora of theories concerning these chemical constituents and their photolysis and chemical reaction products, various chemical compounds have been either hypothesized into existence and model atmospheres have been built around them although they are thermodynamically and structurally impossible.

The purpose of this study is basically double edged. Although at a quick perusal the reader will obviously think that the purpose is a structural study of minor components in planetary atmospheres, which it is, a more subtle objective lies below the surface It is from the author's experience that the methods discussed in this study such as molecular orbital theory lie unfortunately in part to ignorance in the realm of the physical chemist while the qualitative results concern those interested in model atmospheres. The ignorance lies in part to a lack of education but probably even worse to the aura of mystery surrounding these methods. To propose chemical components in atmospheres without any knowledge to whether they are energetically and structurally plausible and to create a model atmosphere around these hypotheses demonstrates a gross lack of scientific methodology. The above example is demonstrated in the problem surrounding the existence of CO_3. In the study of CO_3 there seems to have been little if any interaction between the structural physical chemists and the atmospheric physicists who

were proposing CO_3 as an important intermediate in the Venusian atmosphere. The idea of whether CO_3 was structurally stable or not seems to have never occurred to those most concerned with its applications. The case of CO_3 is in itself minor to the fact that many compounds have been placed in situations which are physically impossible and some astronomers have gone as far as creating the "building blocks" of life from these situations. What is needed is obviously more interaction between those who use the methods for various theoretical purposes and those who apply the results. The topics in this study are by no means closed and the introduction of the various methods discussed opens many intriguing areas of future research.

2. Molecular Structure and Photolysis of CO_3

The existence (or nonexistence) of the elusive CO_3 molecule has centered around the fact that the stoichiometry of the photolysis of CO_2 does not appear to be correct. Whereas the O_2/CO ratio in the products should theoretically be 0.5, experimentally it has been found to vary between 0.0-0.6. Explanations for this variation have ranged from collisional wall processes, ozone formation, and at the moment the formation of CO_3. Of paramount importance to this question is what is the initial step in the photodissociation? Is the initial step

$$CO_2 \xrightarrow{1200\text{-}1700\,A} CO(X^1\Sigma^+) + O(^1D)$$

and what are the interactions of the products? The formation of CO_3 is determined through the mechanism:

$$O(^1D) + CO_2 \rightarrow CO_3^* \rightarrow CO_3 + h$$

where the CO_3 is initially formed in an excited state. CO_2 is regenerated by the mechanism:

$$CO_3 + CO \rightarrow 2CO_2$$

The mechanism has been discussed by Slanger and Black (1970) and is based upon the fact that the three body recombination

$$O(^3P) + CO + M \rightarrow CO_2 + M$$

where M is the third body is too slow.

The importance of this mechanism in applications to planetary

atmospheres is that CO_2 is the principle component of the atmosphere of both Venus and Mars. To explain the recently discovered low concentrations of CO and O_2 and the known CO_2 photodissociation rates as discussed by both Belton and Hunter (1968) and P. Connes, et al. (1968), Hunter and McElroy (1970) proposed the formation of CO_3 to explain the observations. At the same time various experimental studies of CO_3 have been reported. Moll, et al. (1966), Weissberger, et al. (1967) and Arvis (1969) have identified CO_3 by infrared absorption in a solid CO_2 matrix, but attempted studies by mass spectroscopy and gas phase infrared absorption have proved unsuccessful.

The question of the existence of CO_3 in the atmosphere of CO_3 in the atmosphere of both Venus and Mars has been raised upon kinetic grounds by Slanger and Black (1971) on the grounds that if CO is added to CO_2 during photolysis and if a reaction takes place the O (^{3}P) quantum yield should decrease since CO_3 would react by the mechanism

$$CO_3 + CO \rightarrow 2CO_2$$

and O (^{3}P) should not be regenerated as in the proposed decomposition of

$$CO_3 \rightarrow CO_2 + O(^3P)$$

Lack of this effect raises the question of whether the production of CO_3 by the above mechanisms are feasible.

To determine whether CO_3 is energetically stable in the ground state in the gas phase, molecular orbital calculations were performed upon CO_3 using the INDO (Incomplete Neglect of Differential Overlap)

method as developed by Pople et al. (1965, 1965a). The reader is referred to Appendix I for a discussion of the calculations. Two possible structures were tested in the calculations which were proposed by Moll, et al. (1966) and tested previously by Gimarc and Chou (1968) using Extended Huckel Theory. The C_2 structure was found to be considerably more stable than the structure with C_s symmetry.

C_2 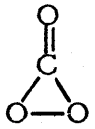 C_s 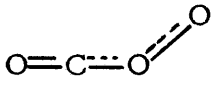

One unexpected result of the INDO calculations reported in Appendix I is the existence of CO_3 as a highly strained ring compound, with the $<$ OCO angle approximately 55° in the ground electronic state The $<$ OCO bond angle from the INDO method is 30° less than that calculated by Gimarc and Chou (1968) using the more approximate Extended Huckel Theory. Highly strained ring systems such as CO_3 are stable under certain conditions, but are highly reactive when compared to their straight chain analogues. In conclusion although CO_3 from a structural analysis should be highly reactive, is energetically a possible reaction intermediate in the photolysis of CO_2 in the atmospheres of both Venus and Mars.

3. Molecular Structure of Free Radicals and Related Compounds in the Venusian Atmosphere

Recent interest in the existence of ClOO has centered around the HCl photodissociation products on Venus in the 50-200 mb. region. As discussed by Prinn (1971) the only primary photodissociation of importance is that of HCl, where the H atoms produced from the dissociation combine with the oxygen (H_2O and O_2 found in the same region) to produce secondary radicals HO_2 and OH and molecular H_2 and H_2O and finally reformed HCl. The ClOO radical is produced from the Cl atoms reacting with O_2 and was first proposed by Porter and Wright (1953) in which they noted that chlorine is an excellent catalyst in the oxidation of CO to CO_2. The cycle of reactions proposed are:

$$Cl + O_2 + M \rightarrow ClOO + M$$

$$ClOO + CO \rightarrow CO_2 + ClO$$

$$ClOO + Cl \rightarrow ClO + ClO$$

$$ClO + CO \rightarrow CO_2 + Cl$$

in which in a steady state process, the cycling yields the net reaction

$$2CO + O_2 \rightarrow 2\,CO_2$$

with Cl atoms acting as catalysts. The importance of the formation of ClOO as an intermediate in the above cycling reactions possible explains the extreme stability of CO_2 in the Venusian atmosphere.

The structure of FOO has been quite extensively discussed by

Jackson (1962), Kasai and Kirshenbaum (1965) and Pimentel et al. (1966). Arkell and Schwager (1967) recently were able to matrix isolate ClOO which has a structure similar to FOO. Both the < ClOO and < FOO bond angles are approximately 110° and the oxygen-oxygen bond distance is 1.225 A. Presented in Appendix II are INDO and CNDO (Complete Neglect of Differential Overlap) molecular orbital calculations for FOO and ClOO radicals in their ground electronic states. The bonding model presented in Appendix II for FOO ClOO and related compounds is similar to that discussed by Sprately and Pimentel.(1966) and Jackson for FOO in which there occurs an interaction between the p orbitals on the halogen atom with one of the π^* anti-bonding orbitals of O_2, the diatomic parent molecule. In both FOO and ClOO electron sharing in the antibonding orbitals of O_2 with the chlorine 3p or fluorine 2p atomic orbitals is an important factor in understanding the bond strengths of these molecules. Discussed in Appendix II in addition to FOO and ClOO are Cl_2O_2, F_2O_2 and $FClO_2$ which have been predicted theoretically by Pimentel and Sprately and the results of the molecular orbital calculations are presented. In conclusion the stability of ClOO in the gas phase as predicted by the molecular orbital calculations along with the work presented by Prinn (1971) makes the existence of ClOO as a stable intermediate as quite reasonable in the photodissociation process of HCl in the Venusian atmosphere.

4. Spectroscopy and Molecular Structure of Polysulfides in the Jovian Atmosphere

Jupiter has regions which are known to exhibit various colors in which the intensity and tone of the colors changes with time. The most prominent colored region is the Great Red Spot but also the North Equatorial Belt (NEB) and the Equatorial Zone (EZ) are known to range in color from dark brown to a bright red-orange. It is difficult to explain production of the colors from the major atmospheric constiuents hydrogen, methane, ammonia and helium. This has resulted in various diverse explanations such as Wildt's (1939) metallic sodium solutions in ammonia, Rice's (1956) trapped free radicals in ammonia clouds and Urey's (1959) discussion of large organic polymers. Lewis and Prinn (1970) have suggested that the observed colors on Jupiter are of inorganic origin produced by photolysis of hydrogen sulfide in regions where ammonia clouds are absent.

If there are breaks in the upper NH_3 cloud layer of Jupiter, such as that suspected in the NEB, permitting the penetration of 2350 A and 2700 A radiation into the Jovian atmosphere, H_2S absorption and photolysis becomes important:

$$H_2S \rightarrow HS + H$$

There exist two major controls upon this process, NH_3 and H_2S photolysis occur at rates some 10^2 to 10^3 times faster than that of CH_4 and one may rule CH_4 out as a primary source of colored complex molecules. The reactions

$$H_2S \rightarrow HS + H$$

$$NH_3 \rightarrow NH_2 + H$$

are of great importance for the production of inorganic rather than organic compounds as discussed by Lewis and Prinn (1970) and they attribute the dark brown coloring of the NEB to these processes. The nature of the coloring matter proposed by Lewis and Prinn (1970) are ammonium and hydrogen polysulfides, $(NH_4)_2\ S_x$ and $H_2\ S_x$ which range in color from yellow to red. Other compounds suggested are N_4S_4 (orange solid) and $N_4S_4H_4$ (colorless solid), also the yellow S_2 biradical investigated by Radford and Rice (1960) and Rice (1956) has been given some attention The NH_3 and H_2S photolysis is occurring in the NH_3 and NH_4HS cloud layers at temperatures of approximately 150°K and 220°K respectively and Lewis and Prinn (1970) have suggested that S_2 and higher sulfur chains could be quite stable in a solid matrix.

Following the suggestion that the coloration of various regions of Jupiter results from the formation of ammonium polysulfides or hydrogen polysulfides, U. V. and visible absorption spectroscopy was carried out upon similar systems. A new method of the preparation of ammonium polysulfides, discussed in detail in Appendix III, was developed utilizing the complexing power of large cations such as the tetra-n-butyl ammonium cation. Upon complexation with S_x^{-2}, produced from $Na_2\ S_x$ a red solid was precipitated. The discussion in Appendix III of the absorption spectra has been broken into three regions, in which the region between 30, 000-45 000 cm^{-1} is of interest to our

discussion of polysulfides in the Jovian atmosphere As discussed by Feher and Munzer (1963) and in Appendix IV the absorptions in this region are due to electronic transitions within the sulfur chains. The unpaired p electrons on the sulfur atoms are in the $3p_4$ and $3p_2$ atomic orbitals and the transition occurring is from these orbitals to the delocalized 3d orbitals upon the sulfur atom. For a more complete discussion of the spectra and structure of ammonium polysulfides the reader is referred to Appendicies III and IV.

Unfortunately except for the narrow band photometry work of Pilcher and McCord (1971) and various other low resolution infrared studies there exists no observational data to compare the experimental laboratory spectra with. The major absorptions as discussed previously for polysulfide molecules occur in the region 30 000-45 000 cm^{-1} (.35-.20μ) and it is in this region narrow band photometry is least sensitive due to Rayleigh scattering. Observing the absorption features in the region between .45 to 8μ it would be extremely difficult to conclude that those features are due to polysulfide or related molecules, since absorption throughout this region occurs for the more abundant CH_4 and NH_3 which would cover quite efficiently the absorption due to the less abundant polysulfides In the near future using a double beam interferometer of .5 cm^{-1} resolution it is hoped that those features due to the polysulfide compounds in the region between .45 to .85μ will be able to be resolved.

5. Molecular Structure of $NH_2NH_2^+$

The radiation from 1650 A to 2300 A penetrates down to the troposphere of Jupiter where it is absorbed principally by NH_3. The primary photolysis reaction is

$$NH_3 \rightarrow NH_2 + H$$

with an insignificant amount of the reaction:

$$NH_3 \rightarrow NH + H_2$$

McNesby (1969) has considered the absorption of wavelengths longer than 1000 A and has discussed qualitatively the photolysis of CH_4 and NH_3. Prinn (1971) has calculated the transmission of wavelengths between 25 A and 2725 A and has obtained the rates of photolysis and the primary photolysis products at each point in the Jovian atmosphere for both CH_4 and NH_3. In discussing the photolysis of NH_3 their exist the possibility of the formation of hydrazine by the reaction:

$$NH_2 + NH_2 \rightarrow NH_2NH_2$$

The first stage in the oxidation of hydrazine, N_2H_3 has not been isolated and only recently the salts of the conjugate acid $N_2H_4^+$ have been isolated, however there exists much evidence that it is an intermediate in the oxidation of hydrazine and perhaps the reduction of hydrogen azide. Organic derivatives of the hydrazyl radical and its conjugate acid have been isolated It has also been suggested that hydrazyl exists in the Jovian atmosphere and may contribute to the colors observed. The $N_2H_4^+$ molecule has been found recently by Reilly and Marquandt (1970)

to be of considerable structural interest since it is an intermediate between the nonplanar hydrazine and the planar ethylene.

In Appendix V, INDO molecular orbital calculations are presented for $N_2H_4^+$. The results of these calculations agree with the projected planar structure. The results obtained by the INDO calculations for the nitrogen isotropic hyperfine coupling constant are in agreement with the ESR data presented by Reilly and Marquardt (1970), Brivati, et. al. (1965), and Edlund and Nilsson (1968). The molecular coefficients of the 1b2g orbital which is localized on the nitrogen p atomic orbitals and the large spin density in these p atomic orbitals agrees with the picture of $NH_2NH_2^+$ of D_{2h} symmetry, with its odd electron placed in the 1b2g from the qualitative molecular orbital diagram of Reilly and Marquardt (1970).

6. Conclusions

The work presented in this thesis has attempted to demonstrate the application of the methods common to theoretical chemistry in understanding the chemical composition of the atmospheres of Jupiter and Venus Due to the limitations of time and the scope of the thesis many areas of research that are opened by using these methods have not been mentioned and in closing I shall briefly discuss a few areas of investigation which deserve attention.

With the development of both high speed computational techniques and the availability of various levels of approximations of molecular orbital theory the investigation of simple chemical reactions by means of these methods has become a field of increasing chemical interest. In the atmosphere of Jupiter with a predominance of simple chemical compounds resulting from simple reactions, the prediction of reaction products, heats of reaction etc would complement the limited observational data An example of the application which would prove useful concerning the ionization of Ch_4. Ab initio molecular orbital calculations in combination with recent data from photon spectroscopy would shed some light upon the structure and spectra of CH_4^+, which possibly is of importance in explaining high resolution infrared spectra of Jupiter. In conjunction with ab initio calculations upon CH_4^+ a program investigating the infrared emission spectra from a methane discharge would be of considerable chemical as well as planetary interest.

Another area of research which merits attention is the investigation of reaction mechanisms concerning simple molecules in interstellar

space. Although at present we have confined ourselves to a program of discovering these simple molecules, some mechanism must exist in which one can arrive at such complex molecules as formaldehyde and cyanoacetolyene from such simple molecules as the hydroxyl radical, water, etc. Application of molecular orbital theory in conjunction with various techniques of experimental spectroscopy would lend themselves in making some sense out of the ever increasing body of observational data.

References

Arkell, A. and I Schwager (1967). J. Am. Chem. Soc. 89, 5999.

Arvis, M. (1969). J. Chim. Phys. 66, 517.

Belton, M. J. S. and D. M. Hunten (1908). Astrophys. J. 152, 731

Brivati, J. A. et al. (1965). J Chem. Soc. 6504.

Connes, P. et al. (1968). Astrophys. J. 152, 731;

Edlund, O. and A. Nilsson (1968). J. Chem. Phys. 49, 749.

Feher, F. and R. Munzer (1963). Chem. Ber. 96, 1131.

Gimarc, B. M. and T. S. Chou (1968). J. Chem. Phys. 49, 4043.

Jackson, R. H. (1962). J Chem. Soc. 4585.

Kasai, P. H. and A. D. Kirshenbaum (1965). J. Am. Chem. Soc. 87, 3069.

Lewis, J. S. and R. G. Prinn (1970). Science, 169, 472.

McElroy, M. B. and Hunten, D. M. (1968). J. Geophys. Res. 75, 1188.

McNesby, J. R. (1969). J. Atmos. Sci. 26, 59.

Moll, N. G. et al. (1966). J. Chem. Phys. 45, 4469.

Pilcher, C. B. and T. B. McCord (1971). Astrophys. J 165, 195.

Pimentel, G. C. and W. L. S Andrews (1966). J. Chem. Phys. 44, 2361.

Pimentel, G. C. and R. D. Spratley (1966). J. Am. Chem. Soc. 88, 2384.

Pople, J. A et al. (1967). J. Chem. Phys. 47, 2026.

Pople, J. A. et al. (1968), J. Am. Chem. Soc. 90, 4201.

Porter, G and F. J. Wright (1952). Z. Electrochem. 56, 782.

Porter, G and F J. Wright (1953). Disc. Faraday Soc. 14, 23.

Prinn, R. G. (1971). J Atmos. Sci. To be published.

Prinn, R G (1971) Paper part of a Ph. D. Thesis presented at M. I. T

Radford, H. E. and F O Rice (1960). J. Chem Phys. 33, 774.

Reilly, M. H. and C. L. Marquardt (1970). J. Chem. Phys. 53, 3257.

Rice, F. O. (1956). J. Chem. Phys. 24, 1259.

Slanger, T G and G. Black (1970). J. Chem. Phys. 53, 3722.

Slanger, T G. and G. Black (1971). J. Chem. Phys. 54, 1889.

Urey, H. C (1959). Hdb. d. Phys 52, 407.

Weissberger, E et al. (1967). J. Chem. Phys. 47, 1764.

Wildt, R. (1939). M N.R A.S., 99, 616.

Appendix No. 1

LCAO-SCF-INDO Calculations on the CO_3 Molecule

LCAO--SCF--INDO Calculations on the CO_3 Molecule

Ira R. Pines

Planetary Astronomy Laboratory
Department of Earth and Planetary Sciences
Massachusetts Institute of Technology

August 1971

Contribution No. 36 of the Planetary Astronomy Laboratory

Abstract

INDO molecular orbital calculations have been performed upon CO_3 in its ground electronic state. Previous extended Huckle calculations have predicted CO_3 to have a C_{2v} structure. INDO calculations predict a three member strained ring of C_{2v} symmetry. A population analysis has been performed upon CO_3 predicting a large overlap population for the C = O bond and a smaller population for the C - O and O - O bonds.

The recent discovery of the low concentration of CO and O_2 in the atmospheres of Venus and Mars in conjunction with the known photodissociation rate of CO_2 has led to the prediction of CO_3 as a stable intermediate in an atmosphere rich in CO_2 [1-5]. Various experimental studies of CO_3 have been reported by Moll et al. [6], Weissberger et al. [7], and Arvis, [8] where CO_3 was identified by infrared absorption in a solid CO_2 matrix. In this paper the structure of CO_3, consisting of 22 valence electrons, shall be reexamined by comparing the qualitative Extended Huckle Theory (EHT) results of Gimarc and Chou [9] with INDO calculations. Evidence shall be presented for the existence of CO_3 as a highly strained three member ring of C_{2v} symmetry.

Method of Calculation

The calculations have been carried out using the Pople-Beveridge-Dobosh [10] Intermediate Neglect of Differential Overlap (INDO). The molecular wave function employed is of an unrestricted form:

$$(1) \quad \Psi = /\psi_1{}^{\alpha}(1)\alpha(1) \ \ldots \ \psi p^{\alpha}(p)\,\alpha(p)\,\psi_i{}^{\beta}(p+1)\beta(p+1) \ \ldots \ \psi q^{\beta}(n)\,\beta(n)/$$

where there are α, ρ and β q electrons ($\rho \geq q$). The unrestricted wave function assigns different electronic

spins to spatially distinct orbitals. For p = q equ. (1) reduces to the restricted wave function [10] which is the case for the ground state of CO_3. In this paper we shall retain the unrestricted formalism and as a matter of convenience consider the wave function of the α electrons. The molecular orbitals are formed from an orthonormal set:

$$(2) \qquad \psi_i^{\alpha} = \sum_{\mu} C_{\mu_i}^{\alpha} \phi_{\mu}$$

for which $C_{\mu_i}^{\alpha}$ are the linear expansion coefficients of

are composed of valence shell Slater Type Orbitals. The F matrices are

$$(3) \quad F_{\mu\mu}^{\alpha} = U_{\mu\mu} + \sum_{\lambda}^{A} [P_{\lambda\lambda}(\mu\mu/\lambda\lambda) - P_{\lambda\lambda}^{\alpha}(\mu\lambda/\mu\lambda)] + \sum_{B\neq A} (P_{BB}-Z_B)\gamma_{AB} \quad (\mu \text{ on atom A})$$

$$(4) \quad F_{\mu\mu}^{\alpha} = (2P_{\mu\nu}-P_{\mu\nu})\ (\mu\nu/\mu\nu) - P_{\mu\nu}^{\alpha}(\mu\mu/\nu\nu) \qquad (\mu\neq\nu) \text{ both on atom A}$$

where: $P_{\mu\nu}^{\alpha} = \sum_{i}^{p} C_{\mu_i}^{\alpha} C_{\mu_i}^{\alpha}$

$$P_{\mu\nu} = P_{\mu\nu}^{\lambda} + P_{\mu\nu}^{\beta}$$

The quantity γ_{AB} is approximated by a Coulomb Integral of the type $(S_A S_A / S_B S_B)$ which involves valence shell s type orbitals upon atoms A and B for which μ and ν are associated. The required one center two electron integrals and the method

of calculating the core integrals $\mu\mu$, which consist of the subtraction of electron-interaction terms from the mean of the ionization potential and electron affinity are listed by Pople et al. [16, 12]. The major difference between the INDO method and the more approximate CNDO (Complete Neglect of Differential Overlap) [13-16] is the retention of one center product $\phi\mu(1)\phi\mu(1)$ involving different atomic orbitals.

Table I presents the parameters employed in the calculations and the equilibrium molecular geometry of CO_3. The calculations were performed on the M.I.T. I.B.M. 360-65 computer, using a program supplied by the Quantum Chemistry Program Exchange [17].

Results and Discussion

A. Gross Molecular Structure

Moll et al. [5] suggest two possible structures for CO_3, preferring the structure of C_{2v} symmetry.

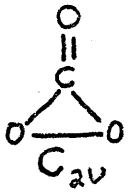

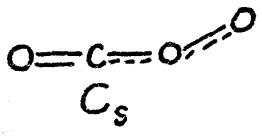

Gimarc and Chou [9] performed E.H.T. calculations on each structure and found the C_{2v} structure most stable. Table II presents the results of the INDO calculations upon the

Table I

INDO Parameters

Orbital	Atom	-1/2 (I+A)*	Z_{eff}*	$\upsilon_{\mu\mu}$*	$\gamma_{\mu\mu}$*
2s	C	14.051	3.150	70.335	10.207
2p	C	5.572	2.800	61.919	10.207
2s	O	25.390	4.400	126.165	13.625
2p	O	9.111	3.950	109.736	13.625

Molecular Geometry

Atom	X(Å)	Y(Å)	Z(Å)
O	0.0	0.0	0.0
C	1.150	0.0	0.0
O	2.390	0.645	0.0
O	2.390	-0.645	0.0

*e.V.

Table II

Species	<C-O-O	Total En. (A.U.)	Electronic En. (A.U.)	Nuclear Repulsion En. (A.U.)	Binding En. (A.U.)	Dipole Moment (D)
$CO_3(C_s)$	116.8°	-59.2410	-115.2289	-55.9827	-1.4351	4.3756
	120.					
	120.0°	-59.2375	-113.8958	-54.6383	-1.4298	4.772
	140.0°	-59.2228	-113.0733	-53.8451	-1.4169	4.8836
	160.0°	-59.1932	-112.4707	-53.2775	-1.3820	5.9400
	180.0°	-58.4232	-111.6617	-53.2385	-0.6120	16.7720
$CO_3(C_{2v})$	LOCO					
	90°	-59.0947	-113.8298	-54.7351	-1.2836	0.1063
	80°	-59.2031	-114.9013	-55.6982	-1.3919	0.5502
	70°	59.3037	-116.1492	-56.8355	-1.4925	0.6978
	65°	-59.3592	-116.7830	-57.4238	-1.65480	0.7898
	60°	-59.4141	-117.7126	-58.2985	-1.6029	0.7897
	57°	-59.4370	-118.3285	-58.8915	-1.6258	0.7612
	55°	-59.4444	-118.8182	-58.3738	-1.6328	0.7087
	52.5°	-59.4379	-119.4830	-59.9451	-1.6267	0.6070

CO_3 (C_s) R_{o-o} = 1.278Å [a] R_{c-o} = 1.33Å $R_{c=o}$ = 1.15Å

CO_3 (C_2) R_{c-o} = 1.40 Å $R_{c=o}$ = 1.15Å

(a) bond lengths from refs.

above structures in which the <OCO and <COO bond angles were varied to find the minimum in the total energy. The most stable structure found was CO_3 of a C_{2v} symmetry with a <OCO bond angle of 55°. The results of Gimarc and Chou, although predicting the same structure as the INDO calculations, are considerably off in their estimation of the LOCO bond angle. A difference of approximately 30° changes the bonding characteristics of CO_3 by reducing the orbital overlap. The reason for the inability of the data of Gimarc and Chou [9] to predict the correct <OCO bond angle lies in an inherent weakness in E.H.T. [18]. The major assumption in E.H.T. is approximating the hamiltonian as a sum of one-electron effective hamiltonians neglecting the nuclear repulsion and electron repulsion energies. The electronic charge distribution of a molecule being determined by a balance between the one-electron attractions and the repulsion terms, causes an accurate prediction of the structure of a molecule when these terms are neglected to be difficult. Also the INDO method unlike the E.H.T. method is based upon an iterative process in which convergence to a solution is allowed when a proper potential is chosen.

B. Eigenvalues and Molecular Coefficients

Table III presents the calculated eigenvalues and

Table III

Eigenvalues and Eigenvectors

(A.U.)	$1a_1$	$2a_1$	$1b_2$	$3a_1$	$1b_1$	$2b_2$	$4a_1$	$5a_1$	$2b_1$	$1a_2$	$3b_2$	$4b_2$	$3b_1$	$5b_2$	$6a_1$	$7a_1$
	-1.9821	-1.7045	-1.1993	-0.9399	-0.9330	-0.8087	-0.7483	-0.7100	-0.6588	0.5048	-0.4818	0.1609	0.1895	0.2501	0.3251	0.4978
O 2s	0.0455	-0.7882	0.0	0.0	-0.3133	0.0	-0.3668	-0.1323	0.0	0.0	0.0	0.0	-0.1769	0.0	0.0	-0.3084
Px	0.0504	-0.2164	0.0	0.0	0.3059	0.0	0.6461	0.3135	0.0	0.0	0.0	0.0	-0.4063	0.0	0.0	-0.4199
Py	0.0	0.0	0.2186	0.0	0.0	-0.7069	0.0	0.0	0.0	0.0	-0.5994	0.0	0.0	0.3035	0.0344	0.0
Pz	0.0	0.0	0.0	-0.4351	0.0	0.0	0.0	0.0	-0.7148	0.0	0.0	0.5774	0.0	0.0	0.0	0.0
C 2s	0.3800	-0.4053	0.0	0.0	0.4070	0.0	0.1165	0.0742	0.0	0.0	0.0	0.0	0.7041	0.0	0.0	0.1042
Px	0.2869	0.3899	0.0	0.0	0.1503	0.0	-0.3147	-0.1087	0.0	0.0	0.0	0.0	0.1614	0.0	0.0	-0.7786
Py	0.0	0.0	0.4095	0.0	0.0	-0.4404	0.0	0.0	0.0	0.0	0.2895	0.0	0.0	-0.7391	-0.0910	0.0
Pz	0.0	0.0	0.0	-0.5323	0.0	0.0	0.0	0.0	-0.2861	0.0	0.0	-0.7967	0.0	0.0	0.0	0.0
O 2s	0.5652	0.0668	0.5849	0.0	-0.2359	0.2926	0.1798	-0.2217	0.0	0.0	-0.0718	0.0	-0.1548	0.0918	0.2423	0.1224
Px	-0.1030	0.0363	-0.0983	0.0	-0.4987	0.2402	0.2667	0.1664	0.0	0.0	-0.5226	0.0	0.3295	-0.3952	-0.0579	-0.1788
Py	-0.2329	-0.0448	0.2012	0.0	0.0752	0.0991	0.2536	-0.5972	0.0	0.0	-0.0157	0.0	0.0912	0.1273	-0.0582	-0.0940
Pz	0.0	0.0	0.0	-0.5135	0.0	0.0	0.0	0.0	0.4512	-0.7071	0.0	0.1810	0.0	0.0	0.0	0.0
O 2s	0.5652	0.0668	-0.5849	0.0	-0.2354	-0.2926	0.1798	-0.2217	0.0	0.0	0.0718	0.0	-0.1548	-0.0918	-0.2423	0.122
Px	-0.1030	0.0363	0.0983	0.0	-0.4987	-0.2402	0.2667	0.1664	0.0	0.0	0.5226	0.0	0.3295	0.3952	0.0579	-0.178
Py	0.2324	0.0448	0.2012	0.0	-0.0752	0.0991	0.2536	0.5972	0.0	0.0	-0.0157	0.0	-0.0912	0.1273	-0.6582	0.094
Pz	0.0	0.0	0.0	-0.5135	0.0	0.0	0.0	0.0	0.4512	0.7071	0.0	0.1810	0.0	0.0	0.0	0.0

and molecular coefficients for CO_3. Applying Koopman's theorem, the calculated ionization potential for CO_3 is ~.4818 AU (10.93 eV) as compared with the value of 13.28 eV calculated by Gimarc and Chou [9]. From the molecular coefficients it may be observed that the $3a_1$ and $2b_1$ orbitals are localized loargely on the oxygen and carbon 2pz orbitals and the $1a_2$ orbital is completely localized on the ring oxygen 2pz orbitals and is nonbinding. The highest occupied molecular orbital, $3b_2$ is slightly antibonding and is localized in the 2py and 2pz orbitals of the oxygen and carbon atoms.

C. Electronic Distribution and Dipole Moments

Table IV presents the population analysis [19,20]. The atomic population analysis reflects the inductive order O>N>Cwith an appreciable negative charge upon the carbon atom. The charge distributions for the C, O, O_a and O_b atoms are:

C: $2s^{1.66}\ 2p_\sigma{}^{.51}\ 2p_\pi{}^{1.32}$ O: $2s^{2.14}\ 2p_\sigma{}^{1.07}\ 2p_\pi{}^{3.0}$

O_a, O_b: $2s^{2.08}\ 2p_\sigma{}^{1.67}\ 2p_\pi{}^{2.39}$

while for neutral O and C atoms both in $^3\pi$ phases of their ground states, the distribution is $2s^2\ 2p_\sigma\ 2p_\pi{}^3$ and $2s^2\ 2p_\sigma\ 2p_\pi$ respectively. It can be observed that the O atom has almost the same electron distribution of a neutral O atom.

and molecular coefficients for CO_3. Applying Koopman's theorem, the calculated ionization potential for CO_3 is ~4818 AU (10.93 eV) as compared with the value of 13.28 eV calculated by Gimarc and Chou [9]. From the molecular coefficients it may be observed that the $3a_1$ and $2b_1$ orbitals are localized loargely on the oxygen and carbon 2pz orbitals and the $1a_2$ orbital is completely localized on the ring oxygen 2pz orbitals and is nonbinding. The highest occupied molecular orbital, $3b_2$ is slightly antibonding and is localized in the 2py and 2pz orbitals of the oxygen and carbon atoms.

C. Electronic Distribution and Dipole Moments

Table IV presents the population analysis [19,20]. The atomic population analysis reflects the inductive order O>N>Cwith an appreciable negative charge upon the carbon atom. The charge distributions for the C, O, O_a and O_b atoms are:

C: $2s^{1.66}\ 2p_\sigma{}^{.51}\ 2p_\pi{}^{1.32}$ O: $2s^{2.14}\ 2p_\sigma{}^{1.07}\ 2p_\pi{}^{3.0}$

O_a, O_b: $2s^{2.08}\ 2p_\sigma{}^{1.67}\ 2p_\pi{}^{2.39}$

while for neutral O and C atoms both in $^3\pi$ phases of their ground states, the distribution is $2s^2\ 2p_\sigma\ 2p_\pi{}^3$ and $2s^2\ 2p_\sigma\ 2p_\pi$ respectively. It can be observed that the O atom has almost the same electron distribution of a neutral O atom.

Table IV

a) Atomic Population Analysis

Atomic Molecular Orbitals

Orbitals	$1a_1$	$2a_1$	$1b_2$	$3a_1$	$1b_1$	$2b_2$	$4a_1$	$5a_1$	$2b_1$	$1a_2$	$3b_2$	Total		
O 2s	0.0063	1.8070	0	0	0.1461	0	0.1253	0.0519	0	0	0	2.1366		
2Px	0.1100	0.1067	0	0	0.1982	0	0.4944	0.2510	0	0	0	1.0713		
2Py	0	0	0.3141	0	0	0.1535	0	0	0	0	0.6248	1.0907	O:	6.2106
2Pz	0	0	0	0.7874	0	0	0	0	1.1246	0	0	1.9120		(-0.2106)
C 2s	0.6378	0.6204	0	0	0.3076	0	0.0228	0.0172	0	0	0	1.6661		
2Px	0.1355	0.2036	0	0	0.0753	0	0.0614	0.0292	0	0	0	0.5050		
2Py	0	0	0.2470	0	0	0.0556	0	0	0	0	0.1680	0.3026	C:	3.4942
2Pz	0	0	0	0.8329	0	0	0	0	0.1876	0	0	1.0205		(+0.5058)
O_aO_b 2S	1.0918	0.0127	0.7672	0	0.0384	0.1008	0.0164	0.0546	0	0	0.0017	2.0841		
2Px	0.4034	0.0055	0.0278	0	0.0788	0.0953	0.1736	0.3548	0	0	0.2321	1.6713		
2Py	0.2565	0.0085	0.2883	0	0.2025	0.0250	0.1603	0.4408	0	0	0.0004	1.1326	O_a, O_b :	6.1487
2Pz	0	0	0	0.4767	0	0	0	0	0.2146	0.5797	0	1.2607		(-0.1487)

b) Overlap Population

Bonds											
O=C	0.0022	1.1446	0.0881	0.2280	0.0998	0.3065	0.0422	0.0263	.2013	0	.1708
Oa-C	0.6058	-0.6840	0.2124	0.2628	0.1015	-0.1743	-0.0869	0.0932	-.0768	0	.1222
O_a-O_b	0.6541	0.0129	-0.3898	0.2244	0.2062	-0.2082	-0.0294	-0.4368	-.0960	0.2359	-.2172
	1.2577	1.0735	-0.0893	0.7153	0.4015	-0.0820	-0.0741	-0.3173	.0284	.2359	.0758

Table V

	X (D)	Y	Z
1)	-0.7128	0.0	0.0
2)	0.0040	0.0	0.0
Total	-0.7087	0.0	0.0

Dipole Moment = 0.7087 Debeyes

The ring oxygen atoms are π acceptors and σ donors while the carbon atom is a π donor and a σ acceptor.

The total overlap population (Table IV) leads to some interesting conclusions. The strongest bond is the C=O bond at the apex of the ring, and the C-O σ bonding overlaps are stronger than the σ bonding overlap on the O-O bond. The O-O bond is strongly σ bonding and π antibonding which should lead to the oxygen-oxygen bond with a minor double bond character. The computed O-O bond distance of approximately 1.29 Å as compared with the O-O bond distance in molecular oxygen of 1.20 Å is in agreement with the above conclusions.

The overall charge distribution of a molecule is reflected by its total dipole moment. The major contributions to the dipole moment are 1) net atomic charge density and 2) the atomic polarization resulting from a mixing of and p orbitals. The contributions 1) and 2) and the total dipole moment are presented in Table VI. The negative dipole moment is defined in the sense of with the vector in the negative x direction along the C = O bond.

D. Ground Electronic States of Three-Member Ring Compounds

Cyclic compounds with three-member rings exhibit severe ring strain and have two choices to accomodate the

bonding. Either the interorbital angles of 109° may be retained which minimizes the interelectronic repulsions, or maximum overlap may be achieved by placing the orbitals coaxial between the nuclei in which high interelectronic repulsions may be tolerated. Compounds such as cyclopropane, cyclopropene, ethylene oxide and diazerine [21, 22], although accepting the later bonding situation and being stable under certain conditions, are highly reactive when compared to their straight-chain analogues.

The three highest filled molecular orbitals of CO_3 are the degenerate 2b, and $1a_2$, and the $3b_2$ have a high electron density in the $2p_\pi$ orbitals of the carbon and oxygen atoms. These three orbitals are especially important since they should be the first ones to take part in a chemical reaction. Since the bond energies are proportional to the bond overlaps, the low overlap population of the C-O and O-O bonds as compared to the C=O bond are in agreement with the easier cleavage and higher reactivity of three-member rings as compared to less-strained systems [23].

Summary

CO_3 in its ground electronic state contains a highly strained three-member ring. The large overlap on the C = O

bond and the small overlaps on the C-O and O-O bonds predict a high chemical reactivity for CO_3. In conclusion CO_3 is a possible intermediate for a reaction in the atmospheres of Venus and Mars and noted by McElroy and Hunten [5].

Acknowledgement

The author wishes to thank Dr. J.S. Lewis for his fruitful advice. This work was supported in part by NASA grant NGL-22-009-521.

References

1. Slanger, T.G., and Black, G., 1970, J. Chem. Phys., 53, 3722.
2. Slanger, T.G., and Black, G., 1971, J. Chem. Phys. 54, 1889.
3. Connes, P., et al., 1968, Astrophys. J., 152, 731.
4. Belton, M.J.S., and Hunten, D.M., 1968, Astrophys. J., 153, 968.
5. McElroy, M.B., and Hunten, D.M., 1970, J. Geophys. Res., 75, 1188.
6. Moll, N.G., et. al., 1966, J. Chem. Phys., 45, 4469.
7. Weissberger, E., et al., 1967, J. Chem. Phys., 47, 1764.
8. Arvis, M., 1969, J. Chim. Phys., 66, 517.
9. Gimarc, B.M., and Chou, T.S., 1968, J. Chem. Phys., 44, 1889.
10. Pople, J.A., et al., 1967, J. Chem. Phys., 47, 2026.
11. Slater, J.C., 1930, Phys. Rev., 36, 57.
12. Pople, J.A. and Beveridge, D.L., 1970, Approximate Moleucular Orbital Theory, McGrawy-Hill Book Co., New York, p. 77.
13. Pople, J.A., et al., 1965, J. Chem. Phys., 43, 5129.
14. Pople, J.A. and Segal, G.A., 1965, J. Chem. Phys., 43, 5136.
15. Pople, J.A. and Segal, G.A., 1966, J. Chem. Phys., 44, 3289.

16. Santry, D.P. and Segal, G.A., 1967, J. Chem. Phys. 47, 158.

17. Quantum Chemistry Program Exchange, Dept. of Chemistry, Indiana University, Bloomington, Ind. 47401.

18. Hoffman, R., 1963, J. Chem. Phys., 39, 1397.

19. Mulliken, R.S., 1955, J. Chem. Phys., 23, 1833, 1841.

20. Mulliken, R.S., 1962, J. Chem. Phys., 36, 3428.

21. Kochanski, E., and Lehn, J.M., 1969, Theoret. Chim. Acta, 14, 281.

22. Clark, D.T., 1968, Theoret. Chim. Acta, 10, 111.

23. Shimizu, K. and Kato, H., 1967, Bull. Chem. Soc. Japan, 40, 756.

Appendix No. 2

LCAO-SCF-INDO/CNDO Calculations on FOO, ClOO, F_2O_2, Cl_2O_2 and $FClO_2$

LCAO-SCF--INDO/CNDO Calculations on FOO, ClOO, F_2O_2, Cl_2O_2 and $FClO_2$

Ira R. Pines

Planetary Astronomy Laboratory
Department of Earth and Planetary Sciences
Massachusetts Institute of Technology

August 1971

Contribution No. 38 of the Planetary Astronomy Laboratory

Abstract

Semi-empirical CNDO/INDO calculations are presented for the ground states of FOO, ClOO, F_2O_2, Cl_2O_2 and $FClO_2$. FOO and ClOO, which are of C_s symmetry, are found to have their odd electron localized mainly on the oxygen p_π orbitals. The ground state of F_2O_2 and $FClO_2$ of C_2 and C_1 symmetry respectively are found to be skew with a dihedral angle of approximately 90°. This is explainable from the fact that the highest M.O.'s are antibonding and twisting the molecules relative to each other which reduces the repulsion energy. Cl_2O_2, which is of C_{2v} symmetry in its ground state is found to have its highest filled M.O. slightly bonding, which lends itself to a possible explanation of why Cl_2O_2 is cis planar.

Introduction

Recent studies of FNO-HNO and F_2O_2-H_2O_2 systems by Linnett [1, 2], Linnett and Rosenbeit [3], Pimentel et al. [4, 5], and Jackson [6] have opened the question of whether other halogen atoms may be substituted in place of fluorine. The principal bonding models are the valence bond model proposed by Jackson [6] which involves substantial contribution from ionic species, and the three center molecular orbital model of both Jackson [6], and Kasai and Kirshenbaum [7]. Both Kasai and Kirshenbaum [7] and Spratley and Pimentel [5] discuss the interaction of the fluorine p orbitals with one of the π^* antibonding orbitals on the oxygen atom in both the FOO and F_2O_2 molecules. Spratley and Pimentel [5] consider the electron sharing in the antibonding orbitals of O_2, the diatomic parent molecule, as an explanation for the bonding, and also couple their arguments with related electronegativity and bond strength data. From these arguments Spratley and Pimentel [5] suggest the existence of various unknown molecules such as Cl_2O_2 and Br_2O_2.

In this paper molecular orbital calculations upon FOO, ClOO, F_2O_2, Cl_2O_2 and $FClO_2$ shall be presented using the CNDO/INDO method. FOO has been studied quite extensively by ESR methods [8-10], and INDO calculations shall

be compared with experimental data. The existence of unsymmetrical ClOO of C_s symmetry, not to be confused with symmetricl OClO of C_{2v} symmetry, was first suggested by Porter and Wright [11, 12] as a reactive intermediate in the gas phase photolysis of Cl_2 and O_2. ClOO was estimated by Benson and Buss [13] to be approximately 4 Kcal/mole more stable than its symmetrical isomer OClO, and the bond dissociation energy D(Cl-OO) was estimated to be = 8±2Kcal. Arkell and Schwager [14] were able to matrix isolated ClOO by photolyzing OClO in an argon matrix. Gole and Hayes [15] attempted nonempirical LCAO-MO-SCF calculations upon FOO and ClOO, however the results obtained did not converge, and the calculations were carried out upon the negative ions of FOO and ClOO. Recently Prinn [16] has given ClOO considerable importance in discussing the HCl photochemistry of the atmosphere of Venus. Both Cl_2O_2 and $FClO_2$ obey the bonding model proposed for F_2O_2 by Pimental and Spratley and their molecular structure in the ground electronic state shall be discussed in this paper.

Method of Calculation

The CNDO/2 (Complete Neglect of Differential Overlap) method has been discussed by Pople et al. [17-19]. In the

CNDO method which may be used for both closed and open shell systems using the unrestricted wave function, the molecular orbital ψ_γ is written as a linear combination of valence atomic orbitals ϕ_μ:

$$(1) \quad \psi_\gamma^n = \sum_\mu \phi_\mu \, C_{\mu\gamma}^n$$

where n refers to spin orbitals of α or β spin in the unrestricted formalism and $C_{\mu\gamma}$ are the molecular coefficients. The self-consistent Hamiltonian Matrix $F_{\mu\nu}$ may be given as:

$$(2) \quad F_{\mu\mu}^n = -\tfrac{1}{2}(I_\mu + A_\mu) + [(P_{AA} - Z_A) - (P_{\mu\mu}^n - \tfrac{1}{2})\gamma_{AA} + \sum_{B \neq A} (P_{BB} - Z_B)\gamma_{AB}]$$

$$F_{\mu\nu}^n = \beta_{AB}^\circ \, S_{\mu\nu} - P_{\mu\nu}^n \, \gamma_{AB}$$

where I_μ and A_μ are the ionization and electron affinity of orbital μ, β_{AB}° is the bonding parameter [17,18], P_{AB} is the bond order matrix give as:

$$(3) \quad P_{AB} + \sum_{\mu\nu} (P_{\mu\nu}^\alpha + P_{\mu\nu}^\beta)$$

$$P_{\mu\nu}^n = 2\sum_\gamma C_{\mu_\gamma} \, C_{\nu_\gamma}$$

orbitals μ are on atom A and ν on atom B, $S_{\mu\nu}$ is the overlap integral between orbitals μ and ν, and γ_{AB} is the electron repulsion integral between orbitals on atoms A and B given as:

$$(4) \quad \gamma_{AB} = \int S_A(1) S_B(2) \frac{1}{r_{12}} S_A(1) S_B(2)$$

where S_A and S_B are S orbitals on atoms A and B.

In the INDO Method (Incomplete Neglect of Differential Overlap) [19, 20] in comparison with CNDO method, the one center atomic exchange integrals are retained. Retaining these one center integrals introduces qualitatively the effect of Hunds Rule, which states that on the same atom electrons in different orbitals shall have lower repulsion energies if the spins are parallel. The resultant effect is to introduce some spin density into the σ system for π odd electron radicals, which leads to a non zero isotropic hyperfine constant (a_N). The elements of the F matrix may be written:

$$F^n_{\mu\mu} = -\tfrac{1}{2}(I_\mu + A_\mu) + \sum_\lambda^A P_{\lambda\lambda}(\mu\mu/\lambda\lambda) - P^n_{\lambda\lambda}(\mu\lambda/\mu\lambda)] + \sum_{B\neq A}(P_{BB}-Z_B)\gamma_{AB}$$

$$F^n_{\mu\nu} = (2P_{\mu\nu} - P^n_{\mu\nu})(\mu\nu/\mu\nu) - P^n_{\mu\nu}(\mu\nu/\nu\nu)$$

$(\mu \neq \nu)$ both on atom A

where the quqntities are similar to the CNDO Method. The isotropic hyperfine coupling constant may be given by the relation:

$$(6) \quad a_N = [\tfrac{4\pi}{3} g\beta\gamma_N h \langle S_z \rangle^{-1} / \phi_{S_N}(R_N)/^2] \rho^{spin}_{S_N S_N}$$

where g is the electronic g factor, β is the Bohr magneton,

γ_n is the gyromagnetic ratio of nucleus N, S_z is the spin angular momentum component, $\phi_{S_n}(R_n)$ are Slater Type S orbitals and ρ^{spin}_{SnSn} is the unpaired electronic population of the valence S orbital [21].

Parameters used in the CNDO/INDO calculations and the molecular geometry are presented in Table I. Calculations on molecules containing chlorine atoms are performed using only the CNDO method. The calculations were performed on the M.I.T. IBM 360-65 computer using a program provided by the Quantum Chemistry Program Exchange [22].

Results and Discussion

A. Gross Molecular Structure

Both FOO and ClOO have 19 valence electrons and each are of C_s symmetry. Following the qualitative development of M.O. Theory proposed by Walsh [23], the outermost valence electron is placed in the 6a' orbital, which is the bent counterpart of the π_μ^* antibonding orbital in molecules of $C_{\infty v}$ symmetry. Being similar to other molecules with 17 to 20 valence electrons, the ground state of FOO and ClOO are bent with an apex angle of approximately 110°. Slight variation of the apex angle causes a negligible change in both the total and binding energies. Although CNDO/INDO are able to predict the O-O bond distances and apex angles (Table I) calculated from experimental

Table I

Parameters Employed in the Calculations

	O	F	Cl
Slater exponent	2.257	2.60	2.033
1/2 (I + A)[a]			
s orbital[b]	25.390	32.272	21.591
p orbital	9.111	11.080	8.708
d orbital			0.977
Bonding parameter (β°)	-31.0	-39.0	-22.33
Core charge	6.0	7.0	7.0

Equilibrium Bond Lengths and Angles

FOO	R_{FO} = 1.177Å	R_{OO} = 1.225Å	<FOO = 110°
ClOO	R_{ClO} = 1.47Å	R_{OO} = 1.225Å	<ClOO = 110°
FOOF	R_{FO} = 1.19Å	R_{O-O} = 1.23 Å	<FOO = 109.5°
			δ[c] = <FOO/<OOF = 90°
ClOOC(Cis)	R_{ClO} = 1.47Å	R_{OO} = 123	<ClOO = 109.5°
FOOCl	R_{FO} = 1.19Å	R_{ClO} = 1.47Å	R_{OO} = 1.23Å
	δ = 90	<FOO = 109.5°	<OOCl = 109.5°

a) The average of the ionization potential and the electron affinity of the valence shell orbital.
b) All values listed are expressed in electron volts.
c) Dihedral angle.

data, the predicted O-F bond distance of 1.575Å found by Jackson [6] in F_2O_2 presents a problem in discussing bond strengths. The Cl-O bond distance used in Table I comes from the microwave study of OClO by Pillai and Curl [24] and this was found to be close to the equilibrium bond distance from variational calculations. Gole and Hayes [15] were not able to achieve convergence in their M.O. calculations upon FOO and ClOO using F-O and Cl-O bond distances of 1.63Å and 1.83Å respectively, probably because these values were taken from matrix isolation data which usually does not reflect the equilibrium bond distances in a single isolated molecule. The O-O bond distance used in all the calculations is consistent with that discussed by Spratley and Pimentel [5] in their study of FOO and F_2O_2.

Table II presents the calculated energies of F_2O_2, Cl_2O_2 and $FClO_2$ in different configurations permitted by varying the dihedral angle of approximately 90°, while Cl_2O_2 is most stable in the planar cis configuration of C_{2v} symmetry.

B. Electron Distribution and Dipole Moment

Table III presents the calculated charge distribution of FOO, ClOO, F_2O_2 Cl_2O_2 and $FClO_2$. The fluorine and chlorine atoms on FOO and ClOO carry a negative charge

Table II

Calculated Energies

Molecule	Total Energy[a]	Electronic Energy	Nuclear Repulsion Energy	Binding Energy	Dipole Moment
FOO(INDO)	-61.2268	-107.6125	46.3867	-0.3852	5.6523
ClOO (CNDO)	-52.5478	-93.8769	41.3291	-0.3372	4.4816
Cis FOOF(INDO)	-88.3946	-176.9651	87.5705	-1.2955	0.0661
Trans FOOF (INDO)	-88.3930	-172.5251	84.1321	-1.2940	0.0000
Skew FOOF (INDO)	-88.4073	-174.3214	85.9141	-1.3082	0.1163
Cis ClOOCl (CNDO)	-69.4654	-147.4853	78.0199	-1.2081	2.0385
Trans ClOOCl (CNDO)	-69.3550	-142.7259	72.3709	-1.0976	0.0000
Skew ClOOCl (CNDO)	-69.3623	-144.2474	74.8857	-1.1050	1.4542
Cis ClOOF (CNDO)	-80.8889	-160.0059	79.1170	-1.1291	1.5132
Trans ClOOF (CNDO)	-80.8649	-154.9358	74.0609	-1.1051	0.7947
Skew ClOOF (CNDO)	-81.0622	-161.2850	80.2128	-1.3025	1.5119

a) All values in Atomic Units (A.U.).

Table III

Calculated Charge Distribution

Molecule	Atom	Electron Population	∫(charge)
FOO	F	7.8450	-0.8450
(INDO)	O	5.5247	+0.4753
	O	5.6302	+0.3698
ClOO	Cl	7.5403	-0.5403
(CNDO)	O	5.7389	+0.2611
	O	5.7208	+0.2792
FOOF	F	7.0878	-0.0878
(INDO)	O	5.9087	+0.0913
	O	5.9115	+0.0885
	F	7.0920	-0.0920
Cis - ClOOCl	Cl	7.0027	-0.0027
(CNDO)	O	5.9978	+0.0022
	O	5.9977	+0.0023
	Cl	7.0017	-0.0017
FOOFl	F	7.0700	-0.0700
(CNDO)	O	5.8983	+0.1017
	O	6.0202	-0.0202
	Cl	7.0115	-0.0115

while the oxygens carry the positive charge with the outer oxygen slightly less positve than the inner oxygen. The charge distribution upon F_2O_2 and Cl_2O_2 reflects the similar electronegativites of the oxygen, fluorine, and chlorine atoms with a slight charge transfer from the oxygen to the fluorine and chlorine atoms. The oxygen atom nearest the fluorine atom in $FClO_2$ carries a positive charge while the other atoms are slightly negative. The electron distributions for Cl_2O_2, ClOO and $FClO_2$ are in contradiction with the predictions using electronegativity data [25], where chlorine is considered less electronegative than oxygen and fluorine. In each of the calculations upong compounds containing chlorine atoms the 3d orbitals were included. The overlap of the 3d orbitals on the chlorine with the 2p orbitals of the oxygen permitted large electron density to be contained in the 3d orbitals. The electron distribution of $FClO_2$ reflects this point extremely well with the oxygen atom nearest the fluorine atom being positively charged, while the other three atoms are slightly negatively charged (greater proportion of the negative charge lies on the fluorine atom).

The overall charge distribution in a molecule is reflected in some measure by th total dipole moment. The major contributions to the dipole moment are: a) the net atomic charge densities, b) the atomic polarization

from a mixing of s and p orbitals, and c) the atomic polarization from a mixing of p and orbitals upon each atom. In Table IV are presented the various contributions to the dipole moment and the total dipole moment. The calculated dipole moment for F_2O_2 in its most stable configuration with a dihedral angle of nearly 90° reflects the small difference in the electronegativities of fluorine and oxygen and differs considerably from the value calculated by Jackson [6] for F_2O_2 of 1.44D. Jackson's [6] data as interpreted by Pimental and Spratley [5] require approximately a transfer of 15% of an electric charge while INDO calculations present a picture of a transfer of less than 10% of an electric charge from the oxygen to the fluorine atom. Also noticeable from the INDO calculations are the large atomic polarizations from a mixing of the 3 p and 3 orbitals when the chlorine atom is considered.

C. Eigenvalues

Table V presents the eigenvalues and molecular coefficients for FOO, ClOO, F_2O_2, Cl_2O_2 and $FClO_2$. Applying the Koopmans theorem [26], the calculated vertical ionization potentials are FOO 12.54 eV, ClOO 12.80 eV, F_2O_2 15.42 eV, Cl_2O_2 12.26 eV, and $FClO_2$ 14.46 eV. Although there exists hardly any experimental data to compare these values to, the value of the first ionization potential of H_2O_2 of

Calculated Contributions to the Dipole Moments (Debyes)

Molecule	Contribution	X	Y	Z	Dipole Moment
FOO	a	5.4945	1.9855	0	
(INDO)	b	-0.2246	0.0581	0	
	total	5.2699	2.0437	0	
					5.6523
ClOO	a	4.3569	1.4995	0	
(CNDO)	b	0.6040	-0.0481	0	
	c	-0.7056	-0.0513	0	
	total	4.2553	1.4063	0	
					4.4816
FOOF	a	-0.0283	0.4690	-0.4983	
(INDO)	b	0.0108	-0.4160	0.3963	
	total	-0.0175	0.0530	-0.1020	
					0.1163
cis-ClOOCl	a	0.0054	0.0300	0	
(CNDO)	b	0.0051	0.6939	-0.0001	
	c	0.0101	1.3143	0.0007	
	total	0.0207	2.0384	0.0006	
					2.0385
FOOCl	a	0.0860	0.0770	-0.3794	
	b	0.1784	0.3388	0.3908	
	c	0.0154	1.0698	-0.0023	
	total	0.2799	1.4857	0.0091	
					1.5119

EIGENVALUES AND EIGENVECTORS FOR ALPHA SPIN — Table V

CLOO (CNDO)

EIGENVALUES---		-2.3114 1a'	-1.7497 1a"	-1.5199 2a'	-1.4278 3a'	-1.3585 4a'	-1.2938 2a"	-1.0727 5a'	-1.0507 3a"	-0.9591 6a'	-0.9452 7a'
CL	S	0.2035	-0.3647	-0.5734	-0.0000	-0.2997	0.6033	0.0000	-0.0959	0.0031	0.0000
CL	PX	0.1644	-0.1594	-0.0356	0.0000	0.0923	-0.3312	-0.0000	0.3205	-0.0136	0.0000
CL	PY	0.0388	0.0713	-0.0723	0.0000	0.1965	0.0463	0.0000	-0.0861	-0.9665	-0.0000
CL	PZ	-0.0000	0.0000	0.0000	-0.1960	0.0000	0.0000	0.4024	0.0000	0.0000	-0.8911
CL	DZ2	-0.0640	0.0464	0.0116	0.0000	-0.0222	0.0758	-0.0000	-0.0347	-0.0025	0.0000
CL	DXZ	-0.0000	0.0000	0.0000	-0.1565	0.0000	-0.0000	0.1015	0.0000	-0.0000	0.1615
CL	DYZ	-0.0000	0.0000	0.0000	-0.0103	0.0000	-0.0000	-0.0209	-0.0000	0.0000	-0.0076
CL	DX-Y	0.0979	-0.0950	0.0009	-0.0000	0.0266	-0.1095	-0.0000	0.1172	-0.0212	-0.0000
CL	DXY	0.0417	0.0688	-0.0565	0.0000	0.1309	0.0341	-0.0000	0.0088	0.0980	0.0000
O	S	0.6986	-0.4356	0.3385	-0.0000	-0.0603	-0.1504	0.0000	-0.1031	-0.0546	-0.0000
O	PX	0.0205	0.2747	0.5091	-0.0000	-0.1106	0.3602	0.0000	-0.5211	0.0233	0.0000
O	PY	0.1995	0.3322	-0.1960	0.0000	0.5666	0.2612	-0.0000	0.2280	0.1185	-0.0000
O	PZ	-0.0000	0.0000	0.0000	-0.7440	0.0000	0.0000	0.5034	0.0000	-0.0000	0.3713
O	S	0.5733	0.6494	-0.2120	-0.0000	-0.3083	-0.1414	0.0000	0.0041	0.0279	0.0000
O	PX	-0.1039	0.1199	0.2999	-0.0000	-0.5146	0.2537	-0.0000	0.6728	-0.1771	-0.0000
O	PY	-0.2167	0.0941	-0.3381	-0.0000	-0.3845	-0.4476	0.0000	-0.2808	-0.0765	-0.0000
O	PZ	-0.0000	-0.0000	0.0000	-0.6192	0.0000	-0.0000	-0.7576	-0.0000	0.0000	-0.2047

EIGENVALUES AND EIGENVECTORS FOR BETA SPIN — Table V

CLOO (CNDO)

EIGENVALUES---		-2.3108 1a'	-1.7494 1a"	-1.4807 2a'	-1.3375 3a'	-1.2835 4a'	-1.2368 2a"	-0.9605 5a'	-0.9434 3a"	-0.4731 6a'	-0.3984 7a'
CL	S	-0.2038	0.3600	0.7119	-0.0848	-0.0000	-0.5314	-0.0035	0.0000	-0.0000	-0.0935
CL	PX	-0.1634	0.1559	-0.0107	0.0386	0.0000	0.4238	-0.0710	0.0000	-0.0000	-0.5856
CL	PY	-0.0376	-0.0767	0.0353	-0.2102	0.0000	0.0552	0.9644	-0.0000	-0.0000	-0.0936
CL	PZ	0.0000	-0.0000	-0.0000	-0.0000	-0.3012	-0.0000	-0.0000	-0.8651	-0.3995	0.0000
CL	DZ2	0.0641	-0.0455	0.0003	-0.0077	-0.0000	-0.0928	-0.0026	0.0000	-0.0000	-0.1244
CL	DXZ	0.0000	0.0000	0.0000	-0.0000	-0.1664	0.0000	0.0000	-0.0505	0.3183	-0.0000
CL	DYZ	-0.0000	0.0000	-0.0000	0.0000	-0.0127	-0.0000	0.0000	0.0242	-0.0236	0.0000
CL	DX-Y	-0.0978	0.0943	-0.0141	0.0164	-0.0000	0.1412	0.0074	0.0000	-0.0000	0.0621
CL	DXY	-0.0420	-0.0709	0.0319	-0.1413	0.0000	0.0422	-0.0911	-0.0000	0.0000	0.1129
O	S	-0.6985	0.4423	-0.3319	0.1693	-0.0000	0.0144	0.0853	-0.0000	0.0000	0.1710
O	PX	-0.0172	-0.2662	-0.4512	0.0459	0.0000	-0.6361	0.0493	-0.0000	0.0000	0.0472
O	PY	-0.2007	-0.3380	0.1042	-0.6538	0.0000	0.0991	-0.1587	0.0000	-0.0000	-0.0682
O	PZ	0.0000	0.0000	0.0000	-0.0000	-0.6461	0.0000	0.0000	-0.0992	0.6709	-0.0000
O	S	-0.5736	-0.6516	0.2409	0.3123	-0.0000	0.0357	-0.0280	0.0000	-0.0000	-0.0070
O	PX	0.0953	-0.0839	-0.0688	0.3270	-0.0000	-0.2174	0.0214	0.0000	-0.0000	-0.6883
O	PY	0.2200	-0.1095	0.3213	0.5140	0.0000	0.2035	0.1430	-0.0000	0.0000	0.3123
O	PZ	0.0000	-0.0000	-0.0000	0.0000	-0.6811	-0.0000	0.0000	0.4886	-0.5371	0.0000

EIGENVALUES AND EIGENVECTORS FOR ALPHA SPIN Table V

FOO (INDO)

EIGENVALUES---		-2.6191	-2.1738	-1.6995	-1.5671	-1.5041	-1.4527	-1.2800	-1.2157	-1.1749	-1.0864
		1a'	1a"	2a'	3a'	4a'	2a"	5a'	3a"	6a'	7a'
F	S	0.5321	-0.6114	-0.4057	0.0000	-0.2898	0.1921	-0.0000	0.0473	0.0161	-0.0000
F	PX	0.2146	-0.0643	0.2734	-0.0000	0.3936	-0.3331	0.0000	-0.3373	-0.2364	0.0000
F	PY	0.0399	0.0797	-0.1405	0.0000	0.3479	0.4342	0.0000	-0.5221	0.6165	-0.0000
F	PZ	0.0000	-0.0000	0.0000	0.4789	-0.0000	-0.0000	0.7352	-0.0000	0.0000	0.4796
O	S	0.6368	0.1258	0.5945	-0.0000	-0.1116	-0.0248	-0.0000	0.0663	0.2652	-0.0000
O	PX	-0.1582	0.3705	0.0882	-0.0000	-0.4208	0.2789	-0.0000	0.2447	0.2405	-0.0000
O	PY	0.1600	0.2664	-0.2563	0.0000	0.3217	0.3964	0.0000	0.0242	-0.4434	0.0000
O	PZ	0.0000	0.0000	0.0000	0.7308	0.0000	0.0000	-0.0309	0.0000	-0.0000	-0.6819
O	S	0.4051	0.6016	-0.5013	0.0000	-0.1035	-0.3855	0.0000	-0.0421	0.0369	-0.0000
O	PX	-0.1222	0.0273	0.0292	-0.0000	-0.5707	-0.0645	0.0000	-0.7351	-0.2013	-0.0000
O	PY	-0.1844	-0.1701	-0.2486	0.0000	0.1028	-0.5247	-0.0000	0.0658	0.4440	-0.0000
O	PZ	0.0000	0.0000	0.0000	0.4865	-0.0000	-0.0000	-0.6772	-0.0000	0.0000	0.5521

EIGENVALUES AND EIGENVECTORS FOR BETA SPIN Table V

FOO (INDO)

EIGENVALUES---		-2.5441	-2.0844	-1.6118	-1.4216	-1.4186	-1.3848	-1.1668	-1.1321	-0.4636	-0.4556
		1a'	1a"	2a'	3a'	4a'	2a"	5a'	3a"	6a'	7a'
F	S	-0.5898	0.5895	0.3998	-0.0000	-0.1426	-0.2639	-0.0027	-0.0000	-0.0000	-0.0765
F	PX	-0.2182	0.0182	-0.3474	0.0000	0.2238	0.5108	0.0414	-0.0000	-0.0000	-0.3348
F	PY	-0.0365	-0.0988	0.2236	0.0000	0.5972	-0.0997	-0.7507	-0.0000	-0.0000	-0.0369
F	PZ	0.0000	-0.0000	0.0000	-0.7055	0.0000	0.0000	-0.0000	0.6590	-0.2607	0.0000
O	S	-0.6237	-0.2369	-0.5522	-0.0000	-0.1098	-0.1488	-0.2150	0.0000	0.0000	0.1751
O	PX	0.1932	-0.3675	0.0079	-0.0000	-0.2860	-0.5485	-0.1242	-0.0000	0.0000	0.0018
O	PY	-0.1500	-0.3024	0.3441	0.0000	0.4465	-0.0476	0.4479	-0.0000	-0.0000	-0.1015
O	PZ	0.0000	0.0000	0.0000	-0.5893	0.0000	0.0000	0.0000	-0.3411	0.7324	-0.0000
O	S	-0.3295	-0.5612	0.4707	0.0000	-0.3615	0.3705	-0.0744	0.0000	0.0000	-0.0013
O	PX	0.1110	0.0222	0.0029	-0.0000	-0.2901	-0.0090	-0.2294	-0.0000	-0.0000	-0.8403
O	PY	0.1831	0.2104	0.1564	0.0000	-0.2546	0.4438	-0.3381	0.0000	0.0000	0.3656
O	PZ	0.0000	-0.0000	0.0000	-0.3937	-0.0000	0.0000	-0.0000	-0.6704	-0.6290	0.0000

EIGENVALUES AND EIGENVECTORS

Table V

CLOOF (CNDO)

EIGENVALUES---		-2.0306	-1.6656	-1.2874	-1.1058	-1.0163	-0.9981	-0.9389	-0.7780	-0.7390	-0.7071	-0.5782	-0.5492	-0.5345
		1a	2a	3a	4a	5a	6a	7a	8a	9a	10a	11a	12a	13a
CL	S	0.1155	-0.2257	0.3574	-0.5507	-0.1724	0.2059	0.5590	0.2732	0.0656	0.0407	0.0422	0.0068	-0.0008
CL	PX	0.0651	-0.0662	-0.0142	-0.0457	0.1324	-0.0985	0.0018	-0.2225	0.1351	0.1027	0.1143	-0.8392	0.0604
CL	PY	0.0812	-0.1473	0.1470	-0.0111	-0.0302	-0.0014	-0.2300	-0.3097	-0.1524	-0.1154	-0.3938	0.2212	-0.0051
CL	PZ	0.0093	0.0132	0.0152	0.0089	0.0861	0.1180	-0.0233	0.0134	0.2501	-0.3735	-0.0131	-0.0702	-0.8735
CL	DZ2	-0.0393	.0580	-0.0371	0.0101	-0.0028	0.0090	0.0521	0.0664	0.0148	0.0124	0.0240	-0.0009	-0.0005
CL	DXZ	0.0077	0.0093	0.0083	0.0027	0.0304	0.0363	-0.0080	0.0060	0.0266	-0.0308	-0.0034	0.0024	0.0590
CL	DYZ	0.0091	0.0123	0.0121	0.0074	0.0598	0.0867	-0.0142	0.0008	0.0999	-0.1235	0.0044	0.0111	0.1871
CL	DX-Y	-0.0194	0.0676	-0.0968	-0.0218	0.0670	-0.0372	0.0950	0.0560	0.0590	0.0384	0.0573	0.0971	-0.0090
CL	DXY	0.0638	-0.0703	0.0020	-0.0187	0.0689	-0.0497	-0.0007	-0.1077	0.0361	0.0235	-0.0819	0.0677	-0.0077
O	S	0.3900	-0.6040	0.3415	0.2558	-0.1454	0.0395	-0.3009	0.0512	0.0079	0.0221	0.1348	-0.0414	-0.0035
O	PX	0.1655	-0.0629	-0.3107	0.0302	0.3172	-0.2047	0.3066	-0.0283	0.3173	0.2151	-0.0800	0.1479	-0.0212
O	PY	-0.0222	0.0518	-0.1220	0.3899	-0.1456	0.0693	-0.0707	0.5333	0.0335	0.0375	0.4674	0.0326	-0.0077
O	PZ	0.0464	0.0623	0.0565	0.0360	0.2702	0.4087	-0.0638	-0.0052	0.4460	-0.5390	0.0183	0.0269	0.4157
O	S	0.6008	-0.1365	-0.5836	-0.1572	-0.1385	-0.0732	0.0356	0.0345	-0.0824	-0.2478	-0.0022	0.0218	0.0497
O	PX	-0.0638	0.3073	-0.1049	-0.2865	-0.3494	0.1519	-0.2155	0.0095	-0.2624	-0.2452	0.0789	-0.1677	0.0319
O	PY	-0.0120	0.0303	-0.0867	0.4284	-0.3428	0.2340	0.2593	0.2335	0.0289	0.0099	-0.6607	-0.2543	0.0316
O	PZ	0.1757	0.2141	0.1398	0.0427	0.2709	0.4706	-0.1008	-0.0311	0.0057	0.3946	-0.0223	0.0336	-0.0672
F	S	0.6003	0.6069	0.3714	0.1018	-0.0484	-0.2248	0.0514	0.0022	0.0025	0.0031	-0.0007	0.0026	-0.0146
F	PX	-0.0891	0.0777	0.0291	-0.1507	-0.5035	-0.2270	-0.2497	-0.0705	0.7032	0.1798	-0.0453	0.0945	0.0423
F	PY	-0.0037	0.0100	-0.0403	0.3027	-0.3493	0.2512	0.4105	-0.6396	-0.0079	-0.0220	0.3609	0.1103	-0.0252
F	PZ	-0.1521	-0.0088	0.2983	0.2155	0.0689	-0.4859	0.2643	0.0429	-0.0634	-0.4095	0.0176	-0.0192	0.0984

EIGENVALUES AND EIGENVECTORS

Table V

CLOOCL (CNDO)

EIGENVALUES---		-1.9097 $1a_1$	-1.3565 $1b_1$	-1.2076 $2a_1$	-0.9672 $2b_1$	-0.9388 $3a_1$	-0.9341 $1b_2$	-0.8654 $4a_1$	-0.6493 $3b_1$	-0.6236 $1a_2$	-0.5959 $4b_1$	-0.5849 $5a_1$	-0.4922 $2b_2$	-0.4531 $6a_1$
CL	S	0.2273	-0.3029	0.5462	-0.0000	0.6013	-0.0790	-0.3255	0.0000	0.1355	0.0849	-0.0000	0.0000	-0.0853
CL	PX	0.1182	0.0267	0.1283	-0.0000	-0.1422	0.2842	0.0577	-0.0000	-0.5918	-0.1476	0.0000	0.0000	-0.5871
CL	PY	0.1365	-0.1714	-0.0119	0.0000	-0.1131	-0.1584	0.3546	-0.0000	0.1259	-0.3687	-0.0000	-0.0000	0.3192
CL	PZ	0.0000	0.0000	0.0000	0.2385	0.0000	0.0000	-0.0000	-0.4108	0.0000	-0.0000	0.6591	0.5672	0.0000
CL	DZ2	-0.0693	0.0421	-0.0297	-0.0000	0.0518	-0.0009	-0.0540	-0.0000	0.0556	0.0448	-0.0000	-0.0000	-0.0648
CL	DXZ	-0.0000	-0.0000	0.0000	0.0835	0.0000	0.0000	-0.0000	0.0100	0.0000	-0.0000	0.0452	-0.0917	-0.0000
CL	DYZ	-0.0000	0.0000	0.0000	0.1405	0.0000	0.0000	-0.0000	-0.1296	-0.0000	0.0000	-0.1146	-0.1574	-0.0000
CL	DX-Y	-0.0275	0.1256	0.0543	-0.0000	0.0191	0.1422	-0.0798	-0.0000	0.0157	0.0935	-0.0000	-0.0000	0.1796
CL	DXY	0.0965	-0.0120	-0.0099	-0.0000	0.0057	0.0807	0.1297	-0.0000	0.1173	-0.0443	-0.0000	-0.0000	-0.0519
O	S	0.6003	-0.5417	-0.2195	0.0000	-0.2676	-0.1863	-0.0269	-0.0000	-0.0770	0.1287	-0.0000	-0.0000	-0.0560
O	PX	0.1894	0.2552	-0.1479	-0.0000	0.0926	0.5588	-0.0846	0.0000	0.2894	-0.0092	-0.0000	-0.0000	-0.0334
O	PY	-0.0675	0.0440	-0.3333	0.0000	-0.1488	-0.1189	-0.4806	-0.0000	-0.0938	0.5529	0.0000	0.0000	0.0525
O	PZ	-0.0000	0.0000	0.0000	0.6453	0.0000	0.0000	-0.0000	-0.5606	0.0000	0.0000	-0.2245	-0.3809	-0.0000
O	S	0.6003	0.5417	-0.2195	0.0000	0.2676	-0.1863	-0.0269	0.0000	-0.0770	-0.1287	0.0000	0.0000	0.0560
O	PX	-0.1894	0.2552	0.1479	0.0000	0.0926	-0.5588	0.0846	-0.0000	-0.2894	-0.0092	-0.0000	-0.0000	-0.0334
O	PY	-0.0675	-0.0440	-0.3333	0.0000	0.1488	-0.1189	-0.4806	-0.0000	-0.0938	-0.5529	-0.0000	-0.0000	-0.0525
O	PZ	-0.0000	-0.0000	0.0000	0.6453	0.0000	0.0000	-0.0000	0.5606	-0.0000	0.0000	-0.2245	0.3809	0.0000
CL	S	0.2273	0.3029	0.5462	0.0000	-0.6013	-0.0790	-0.3255	0.0000	0.1355	-0.0849	-0.0000	-0.0000	0.0853
CL	PX	-0.1182	0.0267	-0.1283	0.0000	-0.1422	-0.2842	-0.0577	0.0000	0.5918	-0.1476	-0.0000	0.0000	-0.5871
CL	PY	0.1365	0.1714	-0.0119	0.0000	0.1131	-0.1584	0.3546	0.0000	0.1259	0.3687	0.0000	0.0000	-0.3192
CL	PZ	0.0000	-0.0000	0.0000	0.2385	0.0000	0.0000	0.0000	0.4108	0.0000	-0.0000	0.6591	-0.5672	-0.0000
CL	DZ2	-0.0693	-0.0421	-0.0297	-0.0000	-0.0518	-0.0009	-0.0540	0.0000	0.0556	-0.0448	0.0000	0.0000	0.0648
CL	DXZ	0.0000	-0.0000	-0.0000	-0.0835	-0.0000	-0.0000	0.0000	0.0100	-0.0000	0.0000	-0.0452	-0.0917	0.0000
CL	DYZ	-0.0000	0.0000	0.0000	0.1405	0.0000	0.0000	-0.0000	0.1296	-0.0000	0.0000	-0.1146	0.1574	0.0000
CL	DX-Y	-0.0275	-0.1256	0.0543	-0.0000	-0.0191	0.1422	-0.0798	0.0000	0.0157	-0.0935	0.0000	0.0000	-0.1796
CL	DXY	-0.0965	-0.0120	0.0099	0.0000	0.0057	-0.0807	-0.1297	-0.0000	-0.1173	-0.0443	-0.0000	-0.0000	-0.0519

Table V

EIGENVALUES AND EIGENVECTORS

FOOF (INDO)

EIGENVALUES---		-2.1316 1a	-1.8864 1b	-1.4960 2a	-1.1541 2b	-1.0072 3a	-1.0047 3b	-0.9980 4a	-0.8398 5a	-0.8355 4b	-0.7553 5b	-0.6240 6a	-0.5741 7a	-0.5697 6b
F	S	0.4318	-0.5582	0.4761	0.3497	-0.0517	-0.0920	0.2676	0.0703	0.0777	-0.0340	0.0036	-0.0154	-0.0056
F	PX	0.0949	-0.0310	-0.1017	0.0268	-0.0715	0.4425	0.0391	-0.4698	-0.3013	-0.4139	-0.4805	-0.0544	0.0549
F	PY	0.1524	-0.1469	-0.0242	-0.3378	0.1120	-0.0181	-0.4665	-0.1014	-0.1941	0.3615	0.1398	-0.2485	-0.0933
F	PZ	0.0070	0.0133	0.0198	-0.0305	-0.5104	-0.0751	-0.1153	-0.4064	0.4905	0.1804	-0.1458	0.1730	-0.4788
O	S	0.5199	-0.2693	-0.3493	-0.4773	0.0589	-0.1866	-0.0692	0.0710	0.1214	-0.2659	-0.1142	0.1682	0.0553
O	PX	0.1199	0.1464	-0.3101	0.1968	-0.1115	0.2795	0.3093	-0.0722	-0.0106	0.0135	0.3954	-0.1114	-0.1314
O	PY	-0.1570	0.2140	-0.1792	-0.0674	-0.0001	-0.3177	0.2344	0.2462	0.2770	-0.2701	-0.1673	0.1998	0.0927
O	PZ	0.0337	0.0567	0.0620	-0.0539	-0.5750	-0.0904	-0.1259	-0.1110	0.1074	-0.0419	0.1574	-0.2442	0.7140
O	S	0.4981	0.3095	-0.3498	0.4746	0.1629	-0.0868	-0.1227	-0.0598	0.1370	0.2655	-0.1141	-0.0464	0.1599
O	PX	-0.1290	0.1272	0.3112	0.1927	0.1839	-0.1881	-0.3460	-0.0759	0.0192	0.0149	-0.3966	0.0790	0.1557
O	PY	-0.0389	0.0549	-0.0560	-0.0526	0.0182	-0.5042	0.2991	-0.1458	-0.1068	-0.0416	-0.2011	-0.7159	-0.2097
O	PZ	0.1426	0.2170	0.1790	-0.0656	-0.3539	-0.0765	-0.1089	0.2186	-0.3248	-0.2718	0.1690	0.0259	-0.2074
F	S	0.3955	0.5793	0.4929	-0.3370	0.1529	0.1345	0.2028	-0.0617	0.0916	0.0352	0.0033	0.0042	-0.0160
F	PX	-0.0897	-0.0383	0.0985	0.0254	0.3915	-0.0589	-0.1520	-0.4346	0.3657	-0.4445	0.4624	-0.1062	0.0327
F	PY	-0.0079	0.0125	-0.0171	-0.0283	0.0222	-0.4297	0.2594	-0.4879	-0.4402	0.1860	0.1828	0.4780	0.1329
F	PZ	-0.1402	-0.1531	0.0242	-0.3217	0.0976	0.2419	0.3964	-0.0812	0.2231	0.3728	-0.1397	-0.0598	0.2538

SPIN DENSITY MATRIX

Table VI

CLOO

		CL_{3s}	P_x	P_y	P_z	DZ2	DXZ	DY2	DX-Y	DXZ	O_{2s}	P_x	P_y	P_z	O_{2s}	P_x	P_y	P_z
CL	S	-0.0012	0.0001	0.0073	0.0000	-0.0017	0.0000	-0.0000	0.0013	0.0010	0.0010	-0.0079	0.0014	0.0000	-0.0004	0.0163	-0.0049	-0.0000
CL	PX	0.0001	0.0376	0.0453	0.0000	0.0004	-0.0000	-0.0000	0.0170	-0.0142	-0.0090	-0.0502	0.0170	-0.0000	-0.0012	0.1486	-0.0543	-0.0000
CL	PY	0.0073	0.0453	0.0084	0.0000	0.0095	-0.0000	-0.0000	0.0002	-0.0100	-0.0136	-0.0071	0.0078	-0.0000	0.0001	0.0664	-0.0280	-0.0000
CL	PZ	0.0000	0.0000	0.0000	0.1554	0.0000	-0.1663	0.0175	0.0000	-0.0000	-0.0000	-0.0000	0.0000	-0.2629	-0.0000	0.0000	-0.0000	0.2164
CL	DZ2	-0.0017	0.0004	0.0095	0.0000	-0.0010	0.0000	-0.0000	0.0002	0.0010	0.0005	-0.0043	0.0006	0.0000	-0.0004	-0.0041	0.0029	-0.0000
CL	DXZ	0.0000	-0.0000	-0.0000	-0.1663	0.0000	0.0307	-0.0026	-0.0000	-0.0000	-0.0000	0.0000	-0.0000	0.1150	0.0000	-0.0000	0.0000	-0.1017
CL	DYZ	-0.0000	-0.0000	-0.0000	0.0175	-0.0000	-0.0026	-0.0001	-0.0000	0.0000	0.0000	0.0000	-0.0000	-0.0115	-0.0000	-0.0000	0.0000	0.0033
CL	DX-Y	0.0013	0.0170	0.0002	0.0000	0.0002	-0.0000	-0.0000	0.0066	-0.0037	-0.0061	-0.0218	0.0101	-0.0000	0.0002	0.0613	-0.0248	0.0000
CL	DXY	0.0010	-0.0142	-0.0100	-0.0000	0.0010	-0.0000	0.0000	-0.0037	-0.0002	0.0045	0.0191	-0.0077	-0.0000	0.0003	-0.0256	0.0093	0.0000
O	S	0.0010	-0.0090	-0.0136	-0.0000	0.0005	-0.0000	0.0000	-0.0061	0.0045	0.0024	0.0251	-0.0084	0.0000	0.0003	-0.0633	0.0234	0.0000
O	PX	-0.0079	-0.0502	-0.0071	-0.0000	-0.0043	0.0000	0.0000	-0.0218	0.0191	0.0251	0.0651	-0.0346	0.0000	-0.0009	-0.2290	0.0936	-0.0000
O	PY	0.0014	0.0170	0.0078	0.0000	0.0006	-0.0000	-0.0000	0.0101	-0.0077	-0.0084	-0.0346	0.0161	-0.0000	0.0000	0.1041	-0.0413	-0.0000
O	PZ	0.0000	-0.0000	-0.0000	-0.2629	0.0000	0.1150	-0.0115	-0.0000	-0.0000	0.0000	0.0000	-0.0000	0.5175	-0.0000	-0.0000	0.0000	-0.3883
O	S	-0.0004	-0.0012	0.0001	-0.0000	-0.0004	0.0000	-0.0000	0.0002	0.0003	0.0003	-0.0009	0.0000	-0.0000	0.0000	-0.0018	0.0009	-0.0000
O	PX	0.0163	0.1486	0.0664	0.0000	-0.0041	-0.0000	-0.0000	0.0613	-0.0256	-0.0633	-0.2290	0.1041	-0.0000	-0.0018	0.7528	-0.2936	-0.0000
O	PY	-0.0049	-0.0543	-0.0280	-0.0000	0.0029	0.0000	0.0000	-0.0248	0.0093	0.0234	0.0936	-0.0413	0.0000	0.0009	-0.2936	0.1134	0.0000
O	PZ	-0.0000	-0.0000	-0.0000	0.2164	-0.0000	-0.1017	0.0033	0.0000	0.0000	0.0000	-0.0000	-0.0000	-0.3883	-0.0000	-0.0000	0.0000	0.2966

SPIN DENSITY MATRIX

Table VI

FOO

		F_{2s}	P_x	P_y	P_z	O_{2s}	P_x	P_y	P_z	O_{2s}	P_x	P_y	P_z
F	S	-0.0004	0.0110	0.0014	0.0000	-0.0072	-0.0140	0.0077	0.0000	0.0000	0.0283	-0.0122	-0.0000
F	PX	0.0110	0.0792	0.0075	0.0000	-0.0438	-0.0307	0.0366	-0.0000	0.0009	0.1763	-0.0738	-0.0000
F	PY	0.0014	0.0075	-0.0013	-0.0000	-0.0022	-0.0022	0.0142	0.0000	0.0002	0.0321	-0.0037	-0.0000
F	PZ	0.0000	0.0000	-0.0000	0.0680	-0.0000	0.0000	0.0000	-0.1910	-0.0000	0.0000	-0.0000	0.1640
O	S	-0.0072	-0.0438	-0.0022	-0.0000	0.0322	0.0164	-0.0156	0.0000	-0.0153	-0.1003	0.0529	-0.0000
O	PX	-0.0140	-0.0307	-0.0022	0.0000	0.0164	-0.0278	-0.0024	0.0000	-0.0065	-0.1038	0.0468	-0.0000
O	PY	0.0077	0.0366	0.0142	0.0000	-0.0156	-0.0024	-0.0145	-0.0000	-0.0187	0.0968	-0.0578	0.0000
O	PZ	0.0000	-0.0000	0.0000	-0.1910	0.0000	0.0000	-0.0000	0.5364	0.0000	-0.0000	0.0000	-0.4607
O	S	0.0000	0.0009	0.0002	-0.0000	-0.0153	-0.0065	-0.0187	0.0000	0.0212	-0.0112	-0.0240	0.0000
O	PX	0.0283	0.1763	0.0321	0.0000	-0.1003	-0.1038	0.0968	-0.0000	-0.0112	0.7777	-0.3249	-0.0000
O	PY	-0.0122	-0.0738	-0.0037	-0.0000	0.0529	0.0468	-0.0578	0.0000	-0.0240	-0.3249	0.1337	0.0000
O	PZ	-0.0000	-0.0000	-0.0000	0.1640	-0.0000	-0.0000	0.0000	-0.4607	0.0000	-0.0000	0.0000	0.3956

15.86 eV in the skew configuration, calculated by Fink and Allen [27] from ab initio calculations reflects that these values are not unreasonable.

The highest molecular orbital on both FOO and ClOO is the 6a' orbital localized almost completely upon the pz orbitals and those d orbitals containing planes in the z direction. The 6a' orbital is slightly antibonding which is in accord with the results from ESR data and their interpretation.

The highest molecular orbitals upon F_2O_2 and $FClO_2$ are the 6b and 13a orbitals respectively. These orbitals are localized mainly on the pz atomic orbitals which are found to be antibonding. This picture agrees well with the fact that both F_2O_2 and $FClO_2$ are in a skew configuration, where the twisting of one-half of the molecule relative to the other half has relieved the repulsion of the antibonding orbitals Cl_2O_2 which is most stable in the Cis configuration has the $6a_1$ orbital as its highest occupied orbital. The $6a_1$ orbital is slightly bonding which along with the overlap of the 3d orbitals on the chlorine with the 2p orbitals of the oxygen atoms explain its planer configuration.

D. Comparison of ESR and INDO Data

In Table VI are presented the spin density matrices of the two odd electron radicals, FOO and ClOO. The data

Table VII

FOO (INDO)

^{19}O and ^{17}O Hyperfine Coupling and Electron Density

Sample	$A^{1}_{^{19}F}$	$A_{^{17}O}$	$A_{^{17}O}$	$a^{2}_{2s_F}$	$a^{2}_{2s_O}$	$a^{2}_{2s_O}$
$^{17}O_2F_2$ (liq)[a]	15.9±0.1	22.4±0.3	14.9±0.5	0.00092	0.014	0.0093
$^{17}OF_2$(liq)[b]	13.5	21.7±2.0				
CF_4-$^{17}O_2$ (liq)[c]	12.83	22.17	14.50			
$^{17}O_2F$ (INDO)	16.56	28.61	18.86	0.0004	0.0322	0.0212

1) All values of A in Gauss.

a) F.E. Welsh et al. J. Mol. Spec. 21, 249 (1966).

b) F.I. Metz et al. "Advances in Chemistry Series" No. 54, p. 202 American Chemical Society, Washington, D.C. 1966.

c) R.W. Fessenden and R.H. Schuler, J. Chem. Phys. 44, 434 (1966).

is in agreement with the observation from the molecular coefficients presented in Table V that the odd electron is localized almost completely on the 2p orbitals of the oxygen atoms. Table VII presents a comparison of the ^{19}F and ^{17}O siotropic hyperfine coupling constants and the electron density upon the 2s atomic orbitals of fluorine and oxygen for INDO and ESR results on FOO. The polarization of the 2s orbital by the 2p orbitals should be sufficient to cause a ^{19}F hyperfine splitting of a magnitude calculated in this paper, but a reliable estimate of the electron densities in the 2s orbitals can not be made. The correlation between ESR and INDO data except for the ^{19}F isotropic hyperfine coupling constant is quite poor. The explanation probably lies in the fact that all the ESR measurements have been taken on FOO in the environment of F_2O_2; F_2O or some similar species, while INDO calculations are performed upon a single isolated molecule, which does not account for environmental effects.

Conclusions

Molecular orbital calculations using the CNDO/INDO approximationg have been carried out upon FOO, ClOO, F_2O_2, Cl_2O_2 and $FClO_2$. The predictions of the ground state for F_2O_2 and FOO is in agreement with both the experimental data and the qualitative arguments of Pimentel and Spratley [5].

The structural predictions for ClOO, Cl_2O_2 and $FClO_2$ although basically similar to their fluorine counterparts involve consideration of the electron density in the orbitals.

Acknowledgement

The author would like to thank Professor John S. Lewis for his fruitful advice. This work was supported in part by NASA grant NGL-22-009-521.

References

1. Linnett, J.W., 1961, J. Am. Chem. Soc. 83, 2643.
2. Linnett, J.W., and Rosenbeit, R.W., 1964, Tetrahedron 20, 53.
3. Linnett, J.W., 1963, J. Chem. Soc. 4663.
4. Andrews, W.L.S., and Pimentel, G.C., 1966, J. Chem. Phys. 44, 2361.
5. Spratley, R.D. and Pimentel, G.C., 1966, J. Am. Chem. Soc. 88, 2384.
6. Jackson, R.H., 1962, J. Chem. Soc. 4585.
7. Kasai, P.H. and Kirshenbaum, A.D., 1965, J. Am. Chem. Soc. 87, 3069.
8. Welsh, F.E., et al., 1966, J. Mol. Spec. 21, 249.
9. Adrian, F.J., 1967, J. Chem. Phys. 46, 1543.
10. Fessenden, R.W., and Schuler, R.H., 1966, J. Chem. Phys. 44, 434.
11. Porter, G. and Wright, F.J., 1952, Z. Electrochem. 56, 782.
12. Porter, G. and Wright, F.J., 1953, Disc. Faraday Soc. 14, 23.
13. Benson, S.W. and Buss J.H., 1957, J. Chem. Phys. 27, 1382.
14. Arkell, A. and Schwager, I., 1967, J. Am. Chem. Soc. 89. 5999.
15. Gole, J.L. and Hayes, E.F., 1970, Int. J. Quantum Chem. 35. 519.

16. Prinn, R.G. 1971 J. Atm. Sci. (to be published).

17. Pople, J.A. et al. 1965, J. Chme. Phys. 43, 5129.

18. Pople, J.A. and Segal, G.A. 1965, J. Chem. Phys. 43, 5136.

19. Pople, J.A. and Segal G.A., 1966, J. Chem. Phys. 44, 3289.

20. Pople, J.A. et al., 1967, J. Chem. Phys. 47, 2026.

21. Pople, J.A. and Beveridge, D.L. Approximate Molecular Orbital Theory, McGraw-Hill Book Co., New York, 1960.

22. Pople, J.A. et al., 1968, J. Am. Chem. Soc. 90, 4201

23. Quantum Chemistry Program Exchange, Dept. of Chemistry, Indiana University, Bloomington, Indiana 47401.

24. Walsh, J., 1953, J. Chem. Soc. 2260.

25. Pillai, M.G.K. and Curl, R.E. Jr., 1962, J. Chem. Phys. 37, 2921.

26. Pauling, L., The Nature of the Chemical Bond, 1960, 3rd Ed., Cornell University,Press, Ithaca, N.Y.

27. Koppmans, T., 1933, Physica 1, 104.

28. Fink, W.H. and Allen, L.C., 1967, J. Chem. Phys. 46, 2261.

Appendix No. 3

Preparation and Spectra of Ammonium Polysulfides

Preparation and Spectra of Ammonium Polysulfides

Ira R. Pines

Planetary Astronomy Laboratory
Department of Earth and Planetary Sciences
Massachusetts Institute of Technology

August 1971

Contribution No. 37 of the Planetary Astronomy Laboratory

Abstract

A new method of preparation of ammonium polysulfides is reported utilizing the complexing power of large cations such as tetra-n-butyl ammonium cation. The absorption spectra in both the near U.V. and the visible regions is reported for tetra-n-butyl ammonium polysulfide in various solvents and their solvent shifts are discussed. The occurrence of an ESR spectrum in certain solvents is attributed to the ability of lone pair electrons on nitrogen or oxygen atoms to take part in SN2 reactions on the sulfur chain.

Introduction

Although polysulfides and sulfanes have been known to exist for almost 200 years, the difficulties in easily preparing these compounds in anything resembling a pure state have remained to the present date. In this paper a new method for the preparation of ammonium polysulfide compounds is introduced. Ammonium polysulfides in ionic equilibrium in solution present an opportunity of studying sulfur chains. Previous studies upon sulfur chains have either been performed by heating molecular sulfur and studying its physical properties with change in chain length as a polymer at and above its critical temperature [1-4], studies of the sulfur chain in a crystal [5,6], or ESR studies of liquid sulfur at and above the critical temperature [7,8]. Gardner and Frankel [7,8] in their paper on ESR spectra of liquid sulfur reported g values and line widths which shall be compared with the ESR spectra of tetra-n-butyl-ammonium polysulfide presented in this paper. Absorption spectra shall be presented of tetra-n-butylammonium polysulfide showing a strong solvent dependence of ν_{max} of absorption, and certain features in the absorption spectra are complementary to the ESR spectra presented.

Experimental

A. Instrumentation

The absorption spectra were recorded on a Cary 14R recording spectrophotometry. Quartz matched absorption cells of various path lengths (0.01 to 1.0 cm) were used. The solvents used were purified and fractionated with particular care taken to remove water from the solvents. The values of ν_{max} reported are accurate to within $\pm 100 cm^{-1}$ unless otherwise indicated.

The ESR measurements were made on a Varian E-3, X-band (9GHZ) spectrometer. The sample tube was made of quartz with an inner diameter of approximately 1mm. Sample weights used were less than 1 mg. Peroxylamine disulfonate was used for the scan calibration and polycrystalline DPPH(g=2.0036) cm a capillary was used as a standard for the g value determination

B. Preparation of Tetra-n-butyl-ammonium polysulfide

The most common method used in the preparation of ammonium polysulfide compounds has been the slow passage of hydrogen sulfide through a suspension of sulfur in aqueous ammonia as described by Bloxam [9]. This method usually renders the products impure through hydrolysis of these solutions, so Thomas and Ridings [10] developed a method that replaced the aqueous medium by an alcoholic medium

and Mills and Robinson [11], using this method, reported the preparation of penta and hepta ammonium sulfides.

The method introduced in this paper in the initial steps follows the procedures developed by both Bloch and Hohn [12] and Feher et al. [1]] for the preparation of polysulfane compounds, but differs in that instead of reducing the Na_2Sx with HCl to a crude oil of H_2S_x ($x \sim 2\text{-}8$) composition, the Na_2Sx is reacted with a tetra-n-butylammonium halide compound in which advantage is taken of the complexing power of the cation. This procedure is analogous to the preparation of polyhalide compounds: cations used for complexing polyhalides have included tetraphenyl ammonium cation as discussed by Mooney [14] and Zaslow and Rundle [15], and tetramethylammonium, which was used to complex I_5^- as discussed by Cristie and Guertin [16].

Na_2Sx was prepared from analytical reagent grade sodium sulfide $Na_2S \cdot 9H_2O$ by dissolving in boiling water and the addition of purified precipitated sulfur powder:

(1) $Na_2S \cdot 9H_2O + (x-1)S \rightarrow Na_2Sx + 9H_2O$

followed by filtration and removal of excess unreacted sulfur. Tetra-n-butyl ammonium chloride, obtained from Eastman Organic Chemical, was dissolved in H_2O and then reacted with the aqueous solution of Na_2Sx from which a dark red solid precipitated out upon cooling:

(2) $Na_2Sx + 2(n - C_4H_9)_4NCl \rightarrow 2NaCl + ((n - C_4H_9)_4N)_2Sx$

The red precipitate was purified by recrystallization from concentrated solution of acetone and then washed with carbond disulfide, toward which the precipitate was unreactive, to remove trace unreacted sulfur.

The method chosen fro the analysis of the precipitate has been discussed by Treadwell [17] and basically is the reduction of the polysulfide to sulf and H_2S, by a strong acid such as HCl. The sulfur is washed and dried and then weighed. The hydrogen sulfide evolved is absorbed in an ammoniacal hydrogen peroxide solution. The sulfuric and sulfurous acids produced are oxidized and excess hydrogen peroxide is expelled. Finally the solution is made acid by addition of HCl and determination of the sulfuric acid as barium sulfate is made. At STP one gram molecule of barium sulfate corresponds to one gram molecule of hydrogen sulfide. The above procedure resulted in the determination of the sulfur per molecule in the range of 5.5 to 7.5 for a series of independent synthesis. The compound was then prepared from stoichiometric quantities of reactants, resulting in approximately uniform number of sulfur atoms per molecule, with a molecular formula of $((n - C_4H_9)N)_2S_6$. It has not been ruled out that a solid solution of various chain lengths with an

average of 6 sulfur atoms has been formed, so in the following discussions a chainlength of 6 sulfur atoms will be considered an average.

Results and Discussion

A. Theoretical Expression for Solvent Effects

The general expression for the solvent induced frequency shift have been developed by McRae [18] and Ooshika [19]. By substituting the refractive index for the sodium D-line (N_D) in place of the refractive index at zero frequency (N_D) and assuming that the quadratic Stark effect is negligible compared to other effects, the expression developed by McRae [18] may be simplified. In this paper the dispersion term which causes a small red shift may be considered negligible and shall be omitted since it is a complex funtion of the spectroscopic properties of the solute and solvent molecules. The simplified McRay expression may thus be written as:

$$(1)\quad \Delta\nu = B\left[\frac{N_D^2-1}{2N_D^2+1}\right] + C\left[\frac{(D-1)}{(D+2)} - \frac{(N_D-1)}{(N_D^2+2)}\right]$$

where B and C are constants which are functions of the molecular volume of the solute molecules and their dipole moments in the electronic ground and excited states. For polar solvents the frequency shift may be expressed by

equation 1 in a simplified form. If for any two polar solvents, a and b, the refractive index as well as the contribution from the dispersion term for each one approximately identical, equation 1 reduces to:

$$(2) \quad \nu_a - \nu_b = \Delta\nu = C\left[\frac{D_a-1}{D_b+2} - \frac{D_b-1}{D_b+2}\right]$$

where ν_a and ν_b are ν_{max} in various solvents, concentration, log of the extinction coefficient, included in Tables I-III. Most of the solvents in Tables I-III are polar but also are hydrogen bonding, and large blue shifts are observed in the case of n-π^* transitions in these ptroton donating solvents. Application of equation 2 to these solvents results in a non-linear relation when $(\frac{D_a-1}{D_a+2} - \frac{D_b-1}{D_b+2})$ is plotted vs. $\Delta\nu(cm^{-1})$ and the calculation of C and the excited state dipole moments is useless from this data. It may be concluded that the observed shifts are mcuh greater in magnitude than expected on the basis of the dielectric constants for these solvents. These large shifts are the result of the proton donation between solute and solvent molecules.

For the different alcohols and nitroalkanes presented in figure 1 and Table I a decreasing blue shift is observed in order of the decreasing electron withdrawing power of the alkyl group. This trend may be related to possible self-association in the alcohols. The equilibrium constants for dimerization of the alcohols increase in order: methanol,

TABLE I

	solvent	$C(M/\ell) \times 10^3$	ν^a_{Max} $(cm^{-1}) \times 10^{-4}$	Log ϵ	N^b_{20}	μ^b (gas)
1	CH_3OH	5.62	23900	2.12	1.3288	1.70
2	C_2H_5OH	5.39	23650	2.15	1.3611	1.69
3	$2\text{-}C_3H_7OH$	3.83	23350	2.27	1.3776	1.66
4	$n\text{-}C_4H_9OH$	3.31	23200	2.39	1.3992	1.66
5	$HOCH_2CH_2OH$	2.21	24500	2.41	1.4314	2.28
6	CH_3NO_2	7.74	22200	2.75	1.3935	3.46
7	$C_2H_5NO_2$	1.92	21800	2.52	1.3918	3.65
8	$2\text{-}C_3H_7NO_2$	2.08	21500	2.65	1.3941	3.77
9	$1\text{-}C_3H_7NO_2$	1.04	21600	2.81	1.4003	3.66
10	$C_6H_5NO_2$	9.07	21450	2.92	1.5562	4.22

a) ± 100 cm^{-1}

b) Refractive indices and dipole moments (μ) from "Handbook of Chemistry and Physics" 49th edition. The Chemical Rubber Co. and from Landolt-Börnstein, "Physikalisch-chemische Tabellen" 5th edition, Springer, Berlin.

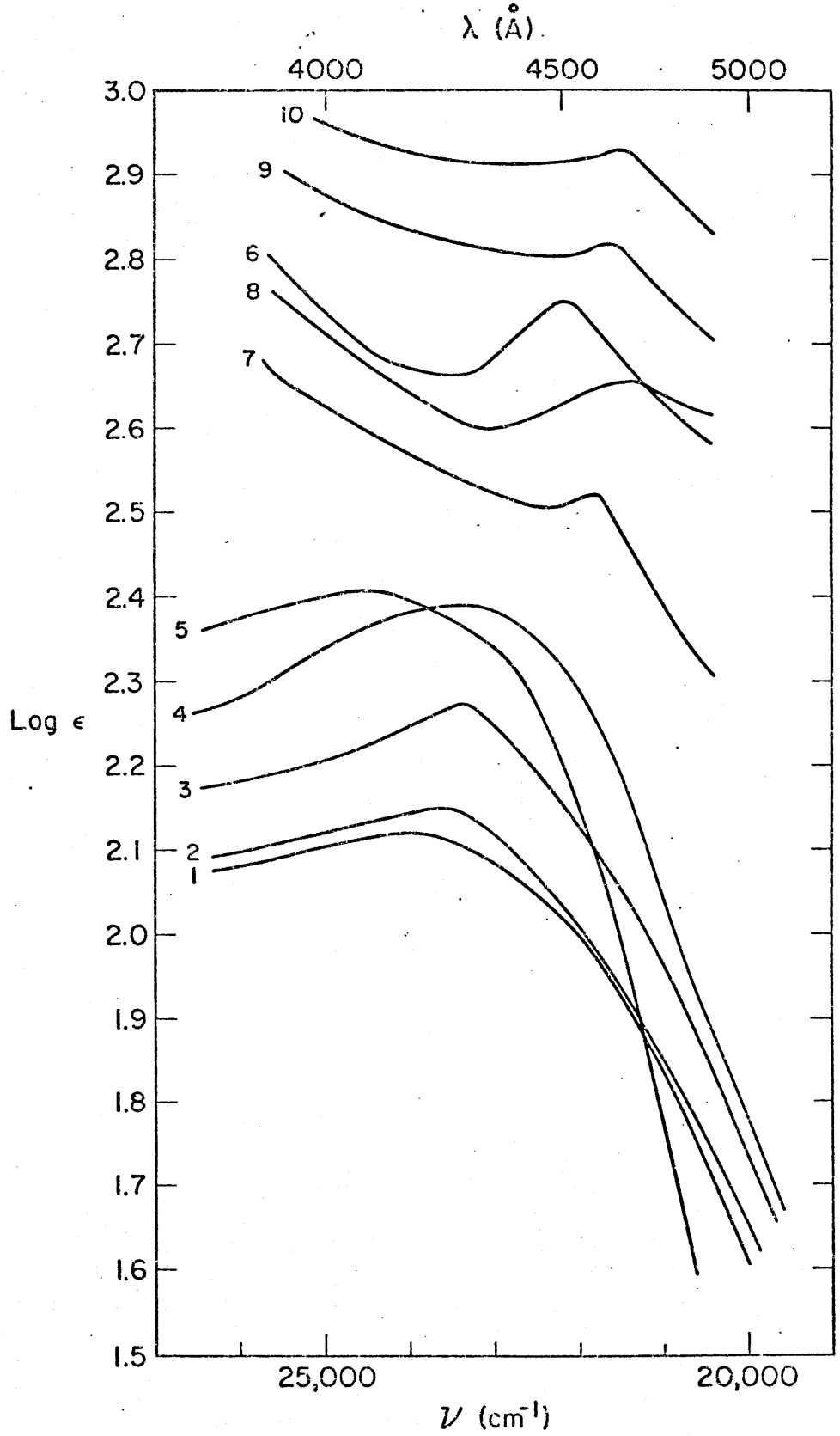
λ (Å)
4000
4500
5000
3.0
2.9
2.8
2.7
2.6
2.5
2.4
2.3
2.2
2.1
2.0
1.9
1.8
1.7
1.6
1.5
Log ε
10
9
6
8
7
5
4
3
2
1
25,000
20,000
ν (cm⁻¹)

FIG. 1

ethanol, isopropyl alcohol and n-butyl alcohol [20]. This trend is consistent with the proton donating ability (acidity) which decreases in the order: methanol, ethanol, isopropyl and n-butyl alcohol. The electromegativities of these alkyl substituents also decrease in the same order. By means of the Taft [21] substituent constant σ^*, for each alkyl group the position of each alcohol may be estimated by the relation

$$(3)\quad (\nu_{max})_{ROH} = (\nu_{max})_{MEOH} + \frac{1.75\ \sigma^*}{2.86 \times 10^{-3}}$$

Table IV presents ν_{max} calculated using Taft's constant and the spectra data. Except for agreement in the direction of the shift there seems to be little correlation between experimental and calculated ν_{max}. A possible explanation is that ammonium polysulfides, being in ionic equilibrium in solution, exhibit a charge transfer spectrum which results in a sizeable red shift which, although it does not alter the relative effect of the alkyl group, changes considerably its magnitude.

Presented in figure 2 and Table II are the absorption spectra and absorption maxima of tetra-n-butylammonium polysulfide in various solvents having absorption bands at 20,500 to 21,500 cm^{-1} and at 16,000 to 17,000 cm^{-1}. The appearance of the absorption band at 16,000 to 17,000 cm^{-1} is associated with the chemical structure of the solvent and has caused a large red shift of ν_{max} for these bands in

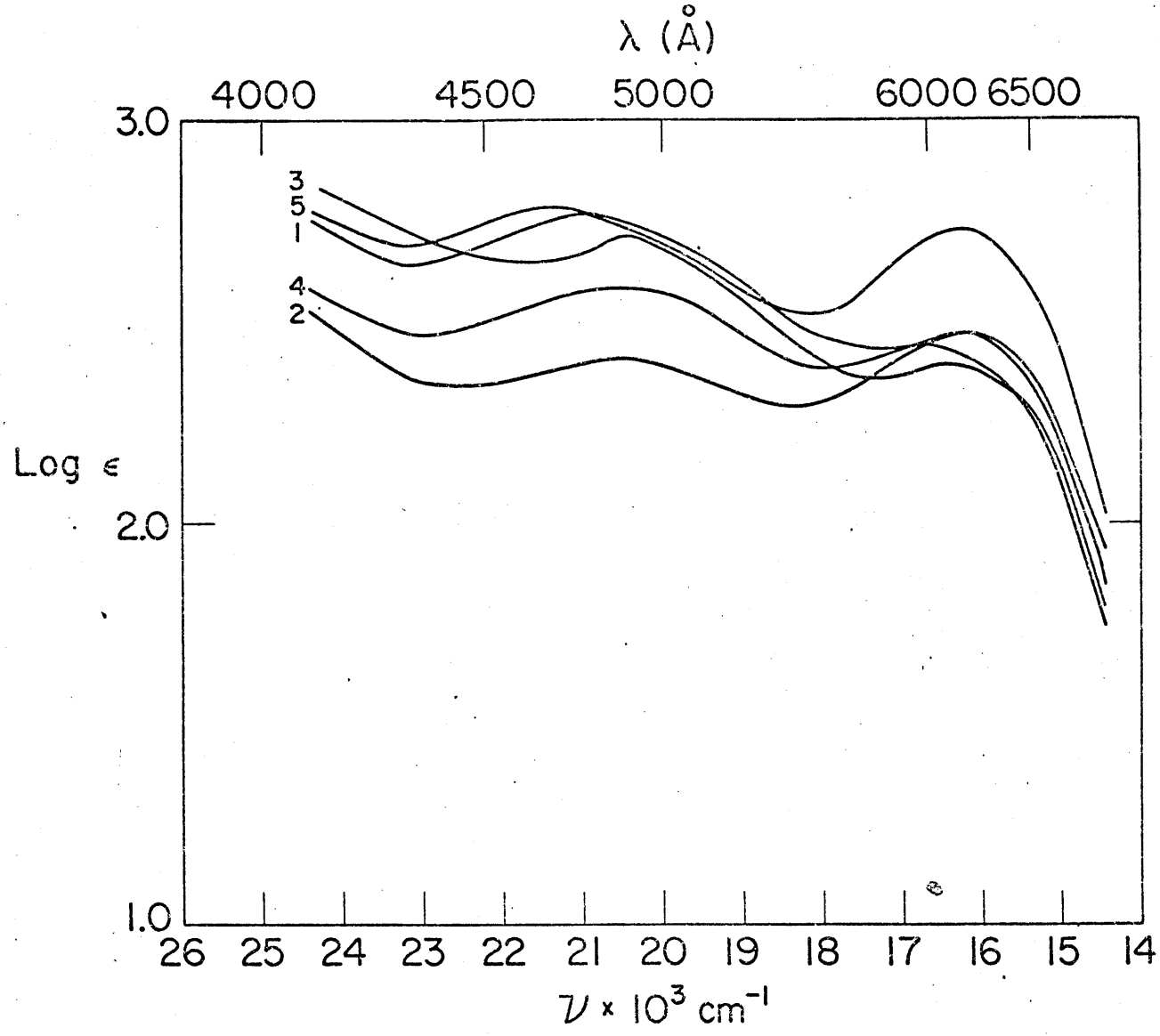
λ (Å)
4000
4500
5000
6000
6500
3.0
2.0
1.0
Log ε
3
5
1
4
2
26
25
24
23
22
21
20
19
18
17
16
15
14
ν × 10³ cm⁻¹

FIG. 2

	solvent	$C(M/\ell)\times 10^2$	ν^a_{Max} $(cm^{-1})\times 10^{-4}$		Log ϵ		$f\times 10^3$		$N^b_{20_d}$	μ^b(gas)
1	acetone	1.78	1.685	2.090	2.45	2.77	3.2	12.1	1.3588	2.88
2	N-N-dimethylacetonide	2.40	1.615	2.055	2.47	2.41	4.05	4.7	1.4351	3.81
3	pyridine	1.69	1.640	2.040	2.39	2.71	3.6	9.8	1.5095	2.19
4	N-N-dimethylformamide	2.60	1.615	2.065	2.47	2.59	3.7	7.9	1.4270	3.82
5	dimethylsulfoxide	6.62	1.625	2.135	2.73	2.79	6.06	12.5	1.4760	3.96

a) ± 100 cm^{-1}

b) Refractive indexes and dipole moments (μ) from "Handbook of Chemistry and Physics" 49th edition. The Chemical Rubber Co. and from Landolt-Börnstein, "Physikalisch-chemische Tabellen" 5th edition, Springer, Berlin.

the region 20,500 to 21,500 cm^{-1} as compared with the spectra in figure 1. This effect will be discussed in the next section of the paper.

B. 16,000 to 17,000 cm^{-1}

The appearance in the region 16,000 to 17,000 cm^{-1} of absorption bands in figure 2 in such solvents as dimethylsulfide (DMSO), acetone, pyridine, N-N-dimethylacetomide, and N-N-dimethyl formanide involve the possibility of complexing of the solvent and solute molecules. Each of these solvents has lone pair electrons which may participate in SN2 reactions at the sulfur-sulfur bond. Examples of these SN2 additions have been reported by Jennen and Hens [22] and Krebs [23] for the reaction of a tertiary amine with molecular sulfur:

$$S_8 + R_3N \rightarrow R_2N^+\text{-S-}S_b\text{-S-}$$

Similar reactions of this type have been noted by Bartlett and Meguerian [24] for the addition of molecular sulfur to triphenyl phosphine.

In solvents such as DMSO a deep blue solution appears, then changes to a colorless solution over a period of days. The deep blue solution and the related ESR spectra to be discussed later in the paper require maintenance of the ionic equilibrium:

$$((C_4Hg)_4N)_2Sx \rightleftarrows 2(C_4Hg)_4N^+ + Sx^{-2}$$

by the polarity of the solvent medium. InDMSO for instance, where the sulfur-oxygen bond has weakened double character, through

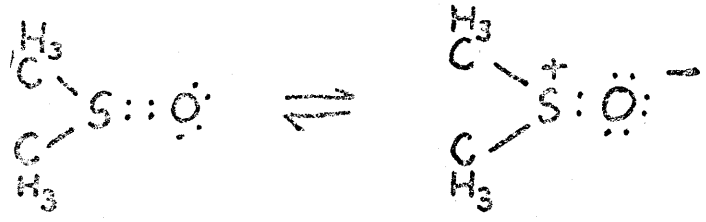

a sharing of electrons with other atoms, as noted by both Pauling [2] and Moffit [26], has a strong polarizing effect along the sulfur-oxygen bond. This may permit the breaking of a sulfur-sulfur bond in the chain resulting in the nucleophilic addition of DMSO to sulfur [27]

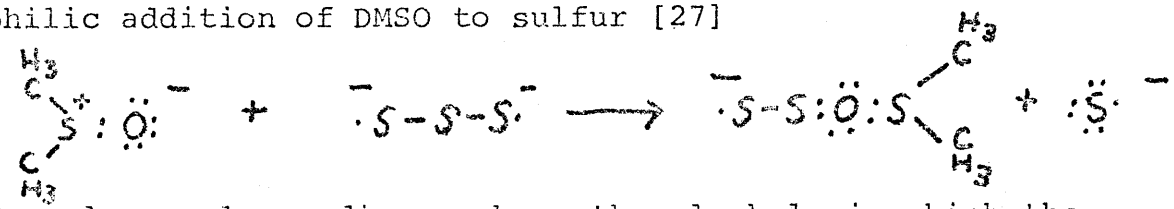

In a less polar medium such as the alcohols in which the oxygen atom is bonded to another atom the polarizing strength of the solvent is weakened, which correlates with the lack of an ESR spectrum in an alcoholic medium. Similar effects appear in the other solvents used in Table II which all have exposed lone pair electron upon the nitrogen or oxygen atoms. In conclusion the appearance of absorption features between 16,000 and 17,000 cm^{-1} is attributable to the maintenance of free radicals in solution by the complexing ability of such solvents as DMSO with exposed lone pair electrons.

C. 30,000 to 45,000 cm^{-1}

The absorption spectra of tetra-n-butylammonium polysulfide in various solvents is presented in figure 3 and the ν_{max} are listed in Table III. The absorptions are due to electronic transitions within the sulfur chain and the explanation is similar to that for electronic spectra of the sulfanes and organic polysulfides, which exhibit similar absorption features in this region. The sulfur atom in its ground state may be pictured as having an electronic configuration $3s^2p^4$. The unpaired p electrons may be place in the 3py and 3pz orbitals and may take part in the formation of b bonds, since the 3s remain relatively undisturbed (3s → 3d ∿ 162 Kcal/mole) while for an unpaired 3p electron the energy of excitation is much less (3p → 3d∿ 49 Kcal/mole). As a result in a molecule that contains more than two sulfur atoms the excitation energy through overlap of the 3d orbitals should be lowered. As noted by Thompson et al. []9] in their M.O. calculations upon the 3d orbitals in sulfur-sulfur binding is quite extensive while contributions from the 4s orbitals are very negligible. Feher et al. [30] in their study of the absorption spectra of polysulfanes found a noticeable red shift and increase in intensity with chain length, and they treated the polysulfanes as a linear chain in which conjugated binding was of major importance. The adoption of the electron gas model

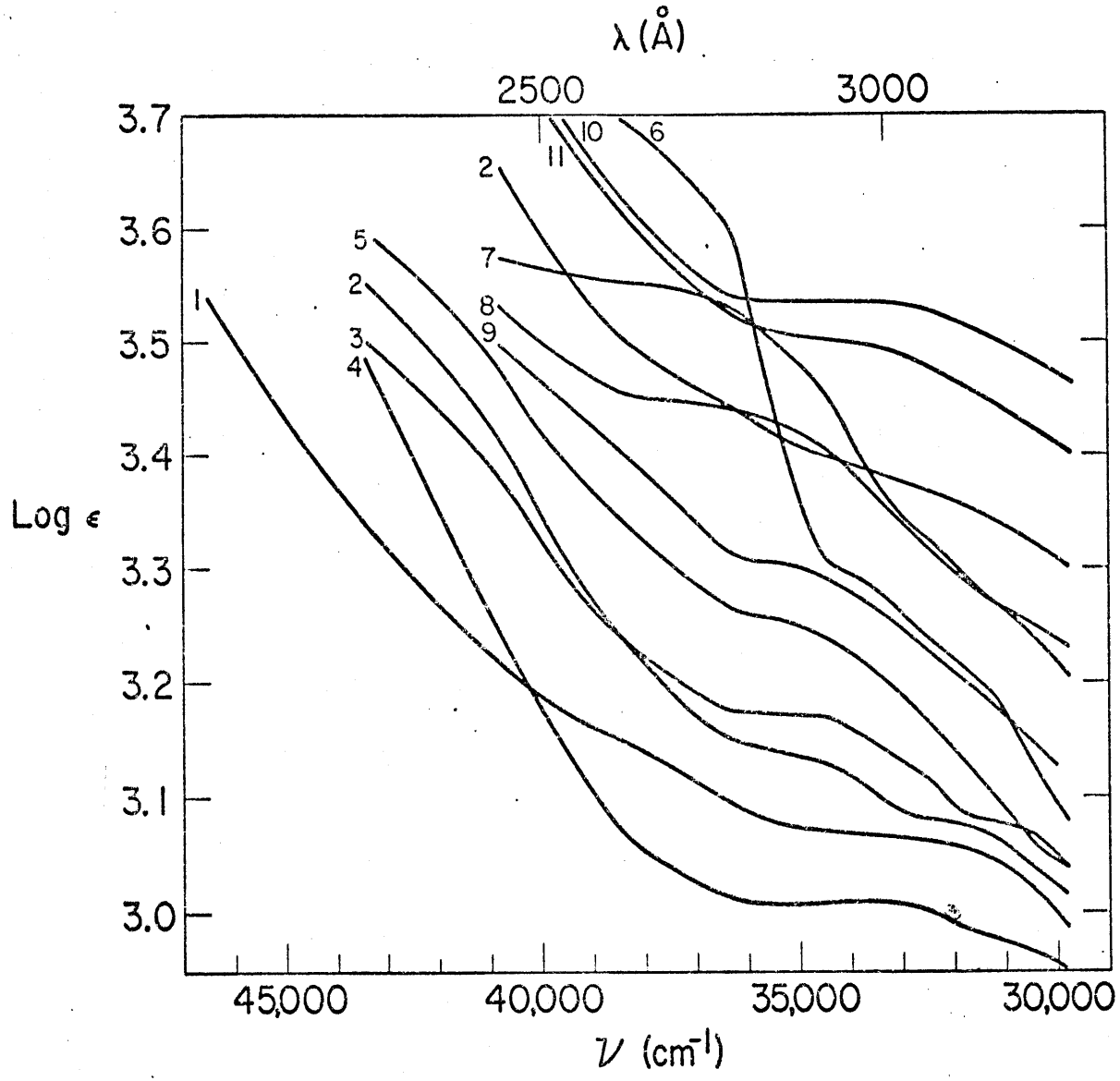
λ (Å)
2500
3000
3.7
3.6
3.5
3.4
3.3
3.2
3.1
3.0
Log ε
1
2
3
4
5
2
6
7
8
9
10
11
45,000
40,000
35,000
30,000
ν (cm⁻¹)

FIG. 3

TABLE III

	solvent	C(M/ℓ)×10²	ν[a](cm⁻¹)			Log ε		
1	CH_3OH	1.78	38000s[b]	32000s		3.135	3.08	
2	C_2H_5OH	2.68	35000s	31500s		3.140	3.075	
3	$I\text{-}C_3H_7OH$	3.18	34500s	31000s		3.175	3.075	
4	$2\text{-}C_3H_7OH$	2.72	34000s	31000s		3.010	2.975	
5	$n\text{-}C_4H_9OH$	3.25	34500s			3.230		
6	CH_3NO_2	.992	36400s	33500s	31250s	3.605	3.375	3.185
7	$C_2H_5NO_2$	1.75	36500s	32500s	31200s	3.527	3.325	3.265
8	$I\text{-}C_3H_7NO_2$	2.41	36000s	31000s		3.430	3.270	
9	$2\text{-}C_3H_7NO_2$	3.43	35000s	31250s		3.300	3.280	
10	N-N-dimethylformamide	.949	32750s			3.500		
11	acetone	1.92	33500s			3.495		
12	N-N-dimethylsulfoxide	1.77	33000s			3.379		

a) all wavelength determinations of shoulders are approximate to ±500 cm^{-1} from the middle of the shoulder.

b) s : shoulder

[31, 32] by Feher et al. [30] in the explanation of the polysulfane spectra was quite successful in predicting absorption maxima.

The $d\pi$-$d\pi$ and $d\pi$-$p\pi$ overlap, although not very strong, contribute to a weak double bond character of the sulfur-sulfur bond [33]. For instance, following Pauling's resonance structure approach, the binding in the sulfur chain may be thought of as intermediate between the simple covalent structure and a polar double bond structure.

The polar double bonded structures have each sulfur atom contributing a d electron to a $d\pi$ electron gas, while the two 3px electrons remain localized on the sulfur atoms. In conclusion the spectra presented in figure 3 are very similar to those presented by Feher et al. [30] for polysulfanes and by Thompson et al. [29] for organic polysulfide, with the electronic transition occurring from the unpaired 3py and $3p_z$ orbitals to a delocalized 3d orbital of the sulfur atom.

ESR Spectra

The ESR spectrum of tetra-n-butyl ammonium polysulfide in DMSO (5.56×10^{-2}M) is presented in figure 4. No attempt was made to obtain a g value more precise than 0.1% and the

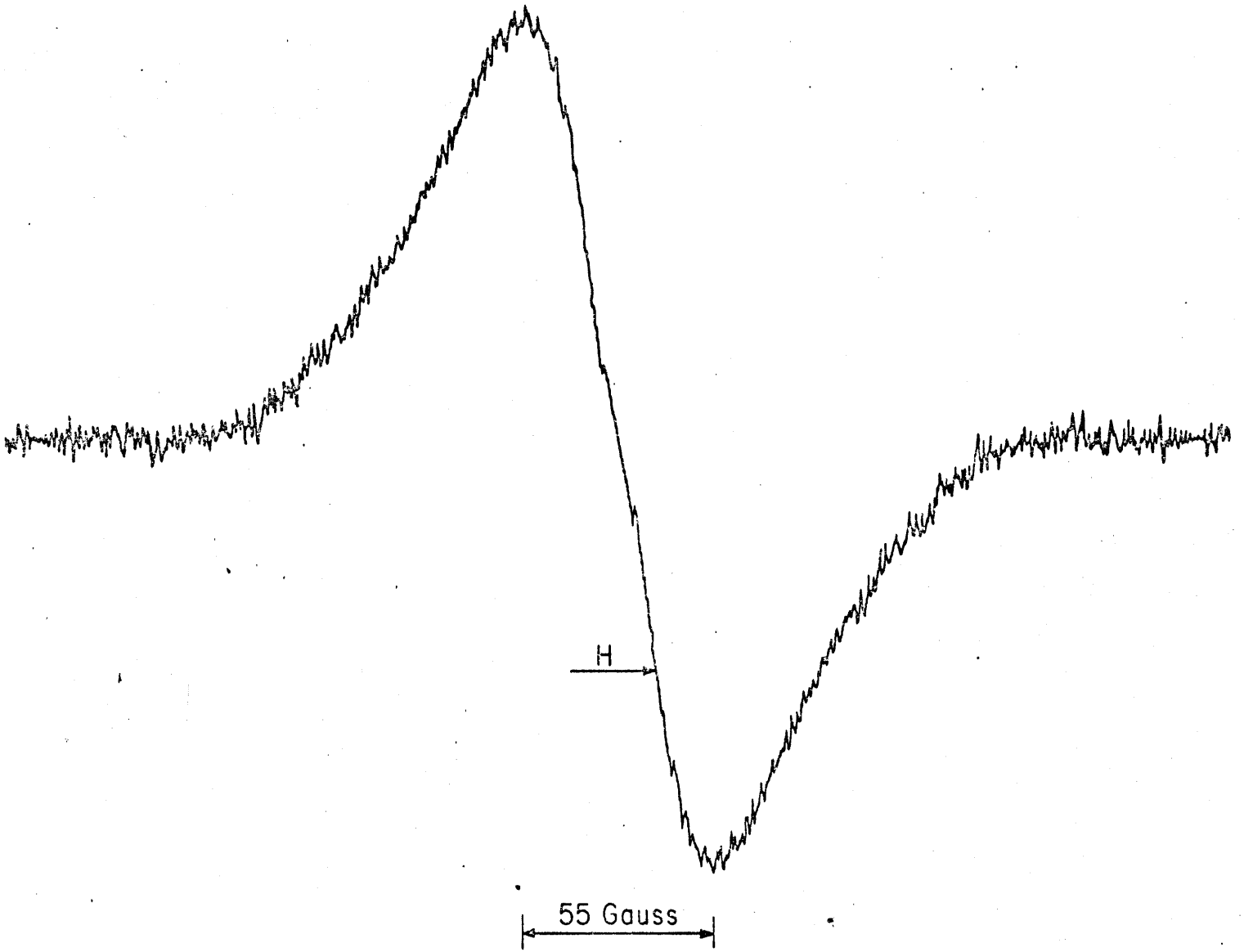

FIG. 4

average value of g was found to be 2.025. The g value reported in this paper is indistinguishable from the value reported by Gardner and Fraenkel [7, 8], g =2.024. The difference from the free electron value of g (2.0023) of 0.023 units is reasonable in considering that the spin orbit coupling increases with atomic number, and for sulfur radicals this difference should be greater than the average value reported for first row organic radicals (~0.004 units).

The line width of the ESR spectrum was observed to 55 Gauss at room temperature. Nuclear hyperfine interactions which would cause broadening in the spectrum, were absent due to the low abundance of ^{33}S (0.76%), the only stable sulfur with a non-zero spin. The values for the line width reported by gardner and Fraenkel [7,8] ranged between 36.1 to 102.4 Gauss for temperatures between 189°C to 414°C. The 55 Gauss width reported in this paper is reasonable when compared to the data on sulfur chains in liquid sulfur. The occurrence of the ESR spectrum in certain solvents has a direct relationship to the absorption spectra taken in these solvents, as has been discussed in section B.

Acknowledgement

The author would like to thank Professor John S. Lewis for many helpful discussions. This work has been partially supported by NASA Grant NGL-22-009-521.

Table IV

Alkyl Group	G*	ν_{max} (Taft)	ν_{max} (Spectra)
CH_3	0	23900	23900
C_2H_5	-.100	23838.2	23650
iso - C_3H_7	-.190	23783.2	23350

1. G. Gee, Trans. Faraday Soc. 48, 515 (1952).

2. F. Fairbrother et al., J. Polymer Sci. 14, 459 (1955).

3. J.A. Pulis et al., Trans Faraday Soc. 58, 474 (1962).

4. J.A. Poulis and W. Derbyshire, Trans Faraday Soc. 59, 559 (1963).

5. S.C. Abrahams and E. Grison, Acta Cryst. 6, 206 (1953).

6. S.C. Abrahams, Acta Cryst. 7, 423 (1954).

7. D.M. Gardner and G.K. Fraenkel, J. Am. Chem. Soc. 76, 5891 (1954).

8. D.M. Gardner and G.K. Fraenkel, J. Am. Chem. Soc. 78, 3279 (1956).

9. T. Bloxam, J. Chem. Soc. 67, 2707 (1895).

10. J.S. Thomas and R.W. Ridings, J. Chem. Soc. 123, 1726 (1923).

11. H. Mills and P.L. Robinson, J. Chem. Soc. 128, 2326 (1928).

12. I. Bloch and F. Hohn,

13. F. Feher et al. Zeit. Anorg. Chem. 255 (1948).

14. R.C.L. Mooney, J. Am. Chem. Soc. 62, 2995 (1940).

15. B. Zaslow and R.E. Rundle, J. Phys. Chem. 61, 490 (1957).

16. K.O. Christie and J.P. Guertin, Inorg. Chem. 4, 905 (1965).

17. F.P. Treadwell, trans. W.T. Hall, Analytical Chemistry vol. II, 7th ed., John Wiley & Sons, New York 1928.

18. E.G. McRae, J. Phys. Chem. 61, 562 (1957).

19. M. Ooshika, J. Phys. Soc. Japan 9, 594 (1954).

20. U. Liddel and E.D. Becker, Spectrochim. Acta 10, 70 (1957).

21. R.W. Taft, Jr., Steric Effects in Organic Chemistry (Edited by M.S. Newman) Chap. 13, John Wiley, New York (1956).

22. A. Jennen and M. Hens, Compt. Rend. 242, 786 (1956).

23. H. Krebs, Gummi u. Asbest 8, 68 (1955).

24. P. Bartlett and G. Meguerian, J. Am. Chem. Soc. 77, 6064 (1955).

25. L. Pauling, J. Phys. Chem. 56, 361 (1952).

26. W.E. Moffitt, Proc. Roy. Soc. (London) A200, 409 (1950).

27. L. Bateman et al., J. Chem. Soc. 2866 (1958).

28. L. Pauling, The Nature of the Chemical Bond, Cornell University Press, 3rd ed., Ithaca, New York 1960.

29. S.D. Thompson et al., J. Chem. Phys. 45, 1367 (1966).

30. F. Feher et al. Chem. Ber. 96, 1131 (1963).

31. H. Kuhn, J. Chem. Phys. 16, 840 (1948).

32. N.S. Baylis, Quart. Rev. 10, 407 (1956).

Appendix No. 4

LCAO-SCF-CNDO Calculations on Sulfur Chains

LCAO-SCF-CNDO Calculations on Sulfur Chains

Ira R. Pines

Planetary Astronomy Laboratory
Department of Earth and Planetary Sciences
Massachusetts Institute of Technology

August 1971

Contribution No. of the Planetary Astronomy Laboratory

Abstract

The total energy, binding energy, electronic energy, and charge distributions of sulfur chains, S_N, N = 2, 3 ...8, were computed using the CNDO/2 method. Calculations on each chain were performed for spin multiplicities of one and three and it was observed that chains with five sulfur atoms or more were stable with a spin multiplicity of three. These results are discussed in relation to the ESR spectra of liquid sulfur and the absorption spectra of the polysulfides.

Introduction

In a previous paper [1] the absorption spectra of tetra-n-butylammonium polysulfide in which the transitions in the region 25-40,000 cm^{-1} were attributed to electronic transitions involving the unpaired electrons on the 2py and 2pz atomic orbitals on the sulfur atom being promoted to delocalized 3d orbitals in the sulfur chain. Previous studies of chain-like sulfur molecules have been carried out by Feher and Munzer [2] on polysulfanes in which a calculated and observed absorption maxima were presented. Thompson et al. [3] performed an all valency molecular orbital calculation upon some organic polysulfides up to the tetra sulfide and concluded that the 3d orbitals were important in sulfur-sulfur bonding in the chain, but the contribution from 4_s electrons was negligible. Spitzer et al. [4] have performed extended Huckel calculations for sulfur chains S_N, N=2, 3...8, sulfanes H_2S_N, N=2, 3...8, and sulfur rings S_N, N = 4,6,8,12 in which the energy levels, charge distributions and other properties have been computed.

In this paper CNDO/2 molecular orbital calculations shall be presented for sulfur chains S_N, N=2, 3...8. A discussion of possible bonding models and their relation to the calculated results shall be presented. Also on argument for a change in stability from singlet to triplet

spin multiplicity, as the chain length is increased shall be presented, including its effect upon the ESR spectra of liquid sulfur and sulfur chains in solution.

Method of Calculation

The method used is the CNDO/2 (Complete Neglect of Differential Overlap) was delveloped by Pople et al. [5-7]. The CNDO/2 method which can be used for closed shell systems or open shell systems in the unrestricted form, the molecular orbitals ψ_γ are written as linear combinations of valence shell atomic orbitals ϕ_μ and ϕ_ν on atoms A and B:

$$\psi_\gamma^n = \sum_r C_{\mu\gamma}^n \phi_\mu$$

where n refers to spin orbitals α or β in the unrestricted calculations and $C_{\mu\gamma}$ are the molecular coefficients of the self-consistent Hamiltonian matrix $F_{\mu\nu}^n$ given as:

$$F_{\mu\mu}^n = -\tfrac{1}{2}(I_\mu + A_\mu) + [(P_{AA} - Z_A) - (P_{\mu\mu}^n - \tfrac{1}{2})]\gamma_{AA} + \sum_{B\neq A}(P_{BB} - Z_B)\gamma_{AB}$$

$$F_{\mu\nu}^n = \beta_{AB} S_{\mu\nu} - P_{\mu\nu}^n \gamma_{AB}$$

where I_μ and A_μ are the ionization and electron affinity of the μth orbital, $P_{\mu\nu}$ is the density matrix:

$$P_{\mu\nu} = 2\sum_i C_{\mu i} C_{\nu i}$$

$S_{\mu\nu}$ is the overlap integral for atomic orbitals ϕ_μ and ϕ_ν:

$$S_{\mu\nu} = \phi_\mu(1)\phi_\mu(1)$$

P_{AA} and P_{BB} are the total electron density associated with atoms A and B. β°_{AB} is the bonding parameter given as

$$\beta^\circ_{AB} = \tfrac{1}{2}(\beta^\circ_A + \beta^\circ_B)$$

where β°_A and β°_B depend upon the nature of atoms A and B and are listed by Pople et al. [6]. γ_{AB} is the electron repulsion integral between orbitals on atoms A and B:

$$\gamma_{AB} = S_A(1)\ S_B(2)\ \frac{1}{r_{12}}\ S_A(1)\ S_B(2)$$

where S_A and S_B are S orbitals on atoms A and B.

Parameters used in the calculations are presented in Table I. The calculations were performed upon the M.I.T. IBM 360-65 computer using a program provided by the Quantum Chemistry Program Exchange [8].

Results and Discussion

A. Gross Molecular Structure

Sulfur chains from previous studies on polysulfide molecules have been found to have unbranched chain-like structures [9-11]. The question of the sulfur chain being coplanar or in a skew configuration still is in doubt. Feher

Table I

Parameters employed in the calculations

	S
	I.816
Slater exponent	
$\frac{1}{2}(I+A)^a$	
S orbital[b]	17.650
p orbital	6.989
d orbital	0.713
Bonding parameter (β°)	-18.150
Core charge	6.0

a) Average of the ionization potential (I) and electron affinity (A).

b) All values of $\frac{1}{2}(I+A)$ in electron volts (eV).

Structural Parameters

	ref	S-S(Å)	<SSS°
S_N N=2...8	1-4	2.04	105

1. C.C. Price and S. Oae Sulfur Bonding, Ronald Press, N.Y.(1962).
2. S.C. Abrahams, Acta Cryst. 8, 661 (1955)
3. J. Donohue and V. Schomaker, J. Chem. Phys. 16, 92 (1948).
4. C.S. Lu and J. Donahue, J. Am. Chem. Soc. 66, 818 (1944).

and Munzer [2] assumed a coplanar zig-zag chain structure in their study of the absorption spectra of the sulfanes. The stable sulfur molecule exists as a symmetrically puckered eight member ring, S_8, in both the orthorhombic and monoclinic crystalline forms [12] as well as in the vapor at ordinary temperatures [13] favoring an azimuthal angle of 103° around the S-S linkage. This data has led Price and Oae [14] to assume that the tri and tetra sulfides have similar skewed configurations.

In Table II is presented the effect of varying the dihedral angle upon the total and binding energies for various configurations in a four-member sulfur chain. The coplanar structure is most stable and this presents two possibilities for bonding in the sulfur chains in which conjugation involving 3d orbitals are made use of. In the first case each sulfur would use its 3p orbitals for overlapping to form π double bonds placing the remaining one electron or a lone pair of electrons in a 3d orbital. The other possibility is that each sulfur may use all the available 3s, 3p and 3d orbitals for sulfur-sulfur bonding. The former case requires no particular angular structure due to the use of 3d orbitals.

B. Eigenvalues and Molecular Coefficients

Presented in Table III-V are the eigenvalues and

Table II

		Dihedral Angle	Total En. (A.U.)	Binding En. (A.U.)	Electronic En. (A.U.)
trans	S_4^{-2}	76°[a,b]	-44.3007	-1.2376	-89.1254
cis	S_4^{-2}	76°	-44.2930	-1.2297	-90.2589
	S_4^{-2}	90°	-44.2952	-1.2319	-89.8696
	S_4^{-2}	0°	-47.8278	-1.3560	-92.2475

a) S.C. Abrahams and E. Grison, Acta Cryst. (1953) 6, 206.

b) S.C. Abrahams, Acta Cryst. (1954) 7, 423.

molecular coefficients for S_2^{-2}, S_3^{-2} and S_4^{-2} each with a spin multiplicity of one. The S_2^{-2} molecule, a typical diatomic molecule of $D_{\infty h}$ symmetry has a molecular orbital pattern similar to oxygen with one exception. In the S_2^{-2} molecule the π bonding orbitals are lower in energy than the $2\sigma g$ bonding orbitals for which the arrangment is the opposite in the oxygen molecule [15, 16]. The S_2 molecule with an internuclear bond distance of 2.1 Å has the arrangement of the π bonding and 2 g bonding orbitals opposite to that for the S_2^{-2} radical, which has an internuclear bond distance of 2.04 Å. Since the S_2 molecule should have a larger ionic core than the S_2^{-2} radical, the p orbital taking part in σ bonding are extended which results in a stabilization of bonding over π bonding. In observing the molecular coefficients for S_2^{-2} the effect of the 3d orbitals taking part in the bonding appears to be quite negligible as compared to the 3p orbitals.

Both S_2^{-2} and S_4^{-2} (multiplicity one) of C_{2h} and C_{2v} symmetry respectively show from their molecular coefficients that the effect of the 3d orbitals upon bonding is considerably smaller when compared to the 3p orbitals. If the assumption drawn from the fact that the molecular coefficients of the 3d orbitals are negligible is correct, then the case in which the 3p orbitals overlap each other

EIGENVALUES AND EIGENVECTORS

Table III

S_2^{-2} (CNDO)

EIGENVALUES---		-0.3358 $1\sigma_g$	-0.0883 $1\sigma_u$	0.1467 $1\pi_u$	0.1467 $1\pi_u$	0.1701 $2\sigma_g$	0.2925 $1\pi_g$	0.2925 $1\pi_g$
S	S	-0.6699	0.6742	0.0000	-0.0000	0.2196	-0.0000	0.0000
S	PX	-0.1975	-0.2003	-0.0000	-0.0000	-0.6507	-0.0000	-0.0000
S	PY	0.0000	-0.0000	-0.3235	0.6036	0.0000	-0.3130	0.6220
S	PZ	0.0000	0.0000	0.6036	0.3235	-0.0000	0.6220	0.3130
S	DZ2	0.0554	0.0367	0.0000	-0.0000	0.0841	0.0000	-0.0000
S	DXZ	-0.0000	-0.0000	0.1553	0.0832	-0.0000	-0.1098	-0.0552
S	DYZ	0.0000	-0.0000	0.0000	0.0000	-0.0000	0.0000	0.0000
S	DX-Y	-0.0959	-0.0636	-0.0000	0.0000	-0.1457	-0.0000	0.0000
S	DXY	0.0000	0.0000	-0.0832	0.1553	0.0000	0.0552	-0.1098
S	S	-0.6699	-0.6742	0.0000	0.0000	0.2196	0.0000	-0.0000
S	PX	0.1975	-0.2003	0.0000	0.0000	0.6507	0.0000	-0.0000
S	PY	-0.0000	0.0000	-0.3235	0.6036	0.0000	0.3130	-0.6220
S	PZ	0.0000	-0.0000	0.6036	0.3235	-0.0000	-0.6220	-0.3130
S	DZ2	0.0554	-0.0367	0.0000	-0.0000	0.0841	-0.0000	0.0000
S	DXZ	-0.0000	-0.0000	-0.1553	-0.0832	0.0000	-0.1098	-0.0552
S	DYZ	0.0000	0.0000	0.0000	0.0000	-0.0000	-0.0000	-0.0000
S	DX-Y	-0.0959	0.0636	-0.0000	0.0000	-0.1457	0.0000	-0.0000
S	DXY	0.0000	0.0000	0.0832	-0.1553	-0.0000	0.0552	-0.1098

EIGENVALUES AND EIGENVECTORS

Table IV

S_3^{-2} (CNDO)

EIGENVALUES---		-0.5375 $1a_1$	-0.3337 $1b_2$	-0.1849 $2a_1$	-0.0118 $3a_1$	-0.0112 $1b_1$	0.0154 $4a_1$	0.1045 $2b_1$	0.1246 $5a_1$	0.1685 $2b_2$	0.1988 $3b_1$
S	S	0.4377	-0.6508	-0.5019	-0.1672	0.0000	-0.2337	-0.0000	0.0471	0.0166	-0.0000
S	PX	0.1782	-0.0549	0.1856	0.2595	-0.0000	0.4508	-0.0000	-0.3265	-0.1854	-0.0000
S	PY	0.0310	0.0490	-0.0651	0.4457	-0.0000	-0.2020	-0.0000	0.4625	-0.6645	-0.0000
S	PZ	0.0000	-0.0000	0.0000	0.0000	0.4446	0.0000	-0.6872	0.0000	0.0000	-0.5228
S	DZ2	-0.0549	0.0122	-0.0301	-0.0457	0.0000	-0.0626	-0.0000	0.0399	-0.0012	-0.0000
S	DXZ	0.0000	0.0000	0.0000	0.0000	0.1597	0.0000	-0.0570	0.0000	0.0000	0.1168
S	DYZ	0.0000	-0.0000	0.0000	0.0000	0.0140	-0.0000	0.0208	0.0000	-0.0000	-0.0140
S	DX-Y	0.0821	-0.0375	0.0680	0.0544	-0.0000	0.1080	0.0000	-0.0656	-0.0626	0.0000
S	DXY	0.0232	0.0339	-0.0378	0.1517	-0.0000	-0.0647	0.0000	0.0201	-0.0021	0.0000
S	S	0.6963	-0.0066	0.5898	-0.1200	0.0000	0.0077	0.0000	0.2199	0.0024	0.0000
S	PX	-0.0975	0.2760	0.1383	-0.3425	0.0000	-0.4439	-0.0000	0.2958	0.0709	-0.0000
S	PY	0.1310	0.2157	-0.1770	0.4161	-0.0000	-0.3674	-0.0000	-0.3691	0.0493	0.0000
S	PZ	0.0000	0.0000	0.0000	0.0000	0.7144	0.0000	-0.0095	0.0000	-0.0000	0.6386
S	DZ2	-0.0753	0.0006	0.0504	-0.0508	0.0000	0.0018	-0.0000	0.1203	0.0024	0.0000
S	DXZ	0.0000	-0.0000	-0.0000	-0.0000	-0.0899	-0.0000	0.2093	-0.0000	-0.0000	0.0719
S	DYZ	-0.0000	-0.0000	0.0000	0.0000	0.1241	-0.0000	0.1640	0.0000	-0.0000	-0.0945
S	DX-Y	0.0021	-0.1633	0.0026	-0.0490	0.0000	0.1238	-0.0000	-0.0656	-0.1959	-0.0000
S	DXY	0.0181	0.0400	0.0083	-0.2046	0.0000	-0.0291	0.0000	-0.2625	0.0416	-0.0000
S	S	0.4508	0.6398	-0.5040	-0.1568	0.0000	0.2399	0.0000	0.0444	-0.0155	-0.0000
S	PX	-0.0726	0.0379	0.0196	-0.5055	0.0000	-0.0757	-0.0000	-0.3605	-0.6842	0.0000
S	PY	-0.1699	-0.0621	-0.1997	-0.1299	0.0000	0.5000	0.0000	0.4165	-0.0139	0.0000
S	PZ	0.0000	0.0000	0.0000	0.0000	0.4638	-0.0000	0.6708	-0.0000	-0.0000	-0.5256
S	DZ2	-0.0557	-0.0108	-0.0306	-0.0431	0.0000	0.0642	0.0000	0.0386	0.0032	-0.0000
S	DXZ	-0.0000	-0.0000	-0.0000	-0.0000	-0.0522	-0.0000	0.0085	-0.0000	0.0000	-0.0146
S	DYZ	-0.0000	-0.0000	-0.0000	-0.0000	-0.1577	-0.0000	-0.0568	0.0000	0.0000	-0.1202
S	DX-Y	-0.0638	-0.0481	-0.0789	0.0275	-0.0000	0.1259	0.0000	0.0647	-0.0524	0.0000
S	DXY	0.0586	-0.0150	-0.0027	0.1636	-0.0000	0.0040	-0.0000	-0.0120	0.0323	0.0000

EIGENVALUES AND EIGENVECTORS

Table V

S_4^{-2} (CNDO)

EIGENVALUES---		-0.6574 $1a_g$	-0.5113 $2a_g$	-0.3514 $1b_u$	-0.2646 $3a_g$	-0.1105 $2b_u$	-0.1017 $4a_g$	-0.1017 $3b_u$	-0.0328 $5a_g$	0.0109 $1a_u$	0.0267 $4b_u$	0.0643 $2a_u$	0.0870 $1b_g$	0.1258 $6a_g$
S	S	-0.3079	0.5254	0.5848	-0.3754	0.0000	-0.1676	0.2398	0.0000	-0.1029	0.0421	0.0000	0.0261	0.0000
S	PX	-0.1358	0.1366	-0.0467	0.1461	-0.0000	0.2560	-0.3477	-0.0000	0.4024	-0.2298	0.0000	-0.0612	0.0000
S	PY	-0.0259	-0.0063	-0.0562	-0.0896	-0.0000	-0.2877	-0.2562	0.0000	0.0854	0.5673	0.0000	-0.6070	0.0000
S	PZ	0.0000	-0.0000	-0.0000	-0.0000	0.3162	-0.0000	-0.0000	-0.5562	-0.0000	0.0000	-0.6128	-0.0000	-0.3982
S	DZ2	0.0443	-0.0367	0.0108	-0.0217	0.0000	-0.0319	0.0595	0.0000	-0.0512	0.0287	0.0000	0.0031	0.0000
S	DXZ	-0.0000	-0.0000	-0.0000	-0.0000	0.1253	-0.0000	-0.0000	-0.1204	0.0000	0.0000	0.0239	-0.0000	0.1066
S	DYZ	0.0000	-0.0000	0.0000	0.0000	0.0149	0.0000	-0.0000	0.0055	0.0000	-0.0000	0.0171	0.0000	-0.0164
S	DX-Y	-0.0623	0.0674	-0.0053	0.0576	-0.0000	0.0696	-0.0817	-0.0000	0.0930	-0.0314	-0.0000	-0.0286	-0.0000
S	DXY	-0.0233	-0.0045	-0.0346	-0.0504	-0.0000	-0.1090	-0.0978	-0.0000	0.0500	0.0773	-0.0000	-0.0222	-0.0000
S	S	-0.5901	0.3672	-0.2552	0.5096	0.0000	0.1566	0.0405	-0.0000	-0.1743	0.1689	0.0000	-0.0565	-0.0000
S	PX	0.0323	-0.2213	-0.1990	0.1402	0.0000	-0.1889	0.4154	0.0000	-0.3859	0.2149	0.0000	0.0256	0.0000
S	PY	-0.1523	-0.0748	-0.1632	-0.1985	-0.0000	-0.4819	-0.1611	0.0000	0.3177	0.0219	-0.0000	0.2688	-0.0000
S	PZ	0.0000	-0.0000	0.0000	-0.0000	0.6015	-0.0000	-0.0000	-0.3770	0.0000	-0.0000	0.2998	0.0000	0.5620
S	DZ2	0.0737	-0.0196	-0.0105	0.0426	0.0000	0.0421	0.0214	0.0000	-0.1005	0.0674	0.0000	-0.0349	-0.0000
S	DXZ	0.0000	-0.0000	-0.0000	0.0000	-0.0408	0.0000	0.0000	0.1761	-0.0000	-0.0000	0.1453	0.0000	0.0517
S	DYZ	-0.0000	-0.0000	-0.0000	0.0000	0.1433	0.0000	-0.0000	0.0548	0.0000	-0.0000	0.1124	0.0000	-0.1061
S	DX-Y	0.0170	0.0865	0.1407	0.0380	0.0000	0.1057	0.0108	-0.0000	0.1141	-0.0393	0.0000	-0.1353	0.0000
S	DXY	-0.0389	-0.0445	0.0001	0.0361	0.0000	0.0234	0.1883	0.0000	0.0555	-0.1858	-0.0000	0.1735	0.0000
S	S	-0.5901	-0.3672	-0.2552	-0.5096	-0.0000	0.1566	-0.0405	-0.0000	-0.1743	-0.1689	0.0000	-0.0565	0.0000
S	PX	-0.0323	-0.2213	0.1990	0.1402	0.0000	0.1889	0.4154	0.0000	0.3859	0.2149	-0.0000	-0.0256	-0.0000
S	PY	0.1523	-0.0748	0.1632	-0.1985	-0.0000	0.4819	-0.1611	-0.0000	-0.3177	0.0219	0.0000	-0.2688	-0.0000
S	PZ	0.0000	0.0000	0.0000	0.0000	0.6015	0.0000	-0.0000	0.3770	0.0000	-0.0000	0.2998	0.0000	-0.5620
S	DZ2	0.0737	0.0196	-0.0105	-0.0426	-0.0000	0.0421	-0.0214	-0.0000	-0.1005	-0.0674	0.0000	-0.0349	0.0000
S	DXZ	-0.0000	0.0000	0.0000	0.0000	0.0408	0.0000	-0.0000	0.1761	-0.0000	-0.0000	-0.1453	0.0000	0.0517
S	DYZ	0.0000	0.0000	0.0000	0.0000	-0.1433	0.0000	0.0000	0.0548	-0.0000	0.0000	-0.1124	-0.0000	-0.1061
S	DX-Y	0.0170	-0.0865	0.1407	-0.0380	0.0000	0.1057	-0.0108	0.0000	0.1141	0.0393	0.0000	-0.1353	-0.0000
S	DXY	-0.0389	0.0445	0.0001	-0.0361	-0.0000	0.0234	-0.1883	-0.0000	0.0555	0.1858	-0.0000	0.1735	-0.0000
S	S	-0.3079	-0.5254	0.5848	0.3754	-0.0000	-0.1676	-0.2398	-0.0000	-0.1029	-0.0421	-0.0000	0.0261	-0.0000
S	PX	0.1358	0.1366	0.0467	0.1461	-0.0000	-0.2560	-0.3477	-0.0000	-0.4024	-0.2298	0.0000	0.0612	0.0000
S	PY	0.0259	-0.0063	0.0562	-0.0896	-0.0000	0.2877	-0.2562	-0.0000	-0.0854	0.5673	-0.0000	0.6070	0.0000
S	PZ	0.0000	0.0000	0.0000	0.0000	0.3162	0.0000	-0.0000	0.5562	-0.0000	-0.0000	-0.6128	-0.0000	0.3982
S	DZ2	0.0443	0.0367	0.0108	0.0217	-0.0000	-0.0319	-0.0595	-0.0000	-0.0512	-0.0287	0.0000	0.0031	0.0000
S	DXZ	0.0000	-0.0000	-0.0000	-0.0000	-0.1253	-0.0000	0.0000	-0.1204	0.0000	0.0000	-0.0239	-0.0000	0.1066
S	DYZ	-0.0000	0.0000	-0.0000	0.0000	-0.0149	-0.0000	0.0000	0.0055	-0.0000	-0.0000	-0.0171	-0.0000	-0.0164
S	DX-Y	-0.0623	-0.0674	-0.0053	-0.0576	0.0000	0.0696	0.0817	0.0000	0.0930	0.0314	-0.0000	-0.0286	-0.0000
S	DXY	-0.0233	0.0045	-0.0346	0.0504	0.0000	-0.1090	0.0978	0.0000	0.0500	-0.0773	0.0000	-0.0222	0.0000

to form π double bonds placing the remaining electron or lone pair electrons in the d orbital seems most plausible. Since there exists still a small contribution from the 3d orbitals to the bonding, an additional contribution from a hydridization of 3s, 3p and 3d orbitals resulting in a specific angular arrangement about the S-S linkage also seems quite plausible.

C. Spin Multiplicity and Electron Distribution

Gardner and Fraenkel [17,18] in their study of the paramagnetic resonance of liquid sulfur from 189°C to 414°C were only able to determine a single resonance line at all temperatures which they attributed to either a radical combination reaction:

$$---S\cdot + \cdot S--- \rightarrow ---S-S---$$

or a radical displacement reaction:

$$---S\cdot + ---S-S--- \rightarrow ---S-S---+ \cdot S---$$

Similar spectra for solid sulfur dissolved in CS_2 was observed by Pinkus and Piette [19]. The nature of the resonance line in both liquid sulfur and sulfur chains of various lengths is determined by the interaction of the 2 unpaired electrons on the end sulfur atoms. If the two unpaired electrons are separated by great lengths and

covalent bonds, as in the case of such biradicals as the binitroxides and the chichibabin radical, the interaction is small, and the nature of the ESR spectra is determined by how closely the electrons may approach each other [20-22].

Presented in Table VI are the various energies for sulfur chains of spin multiplicities one and three. Sulfur chains consisting of five or more members appear to be more stable in the state with a multiplicity of three, while sulfur chains with four or less sulfur atoms appear to be most stable in the singlet state. It is important to observe that as the length of the sulfur chain is increased and the electron interaction is decreased, the probability of finding the odd electrons on the end sulfur atoms parallel to each other increases. Sulfur chains with four or less atoms show a tendency to have the odd electrons on the end sulfurs coupled to each other in a anti-parallel direction. Presented in Table VII is the electron distribution for sulfur chains of various lengths and of the most stable multiplicity. Although in each chain of different lengths, the density of electrons is greatest upon the end sulfur atoms, there is a tendency to have more delocalization of the electrons as the chain length is increased.

The absence of fine structure in the ESR spectra of

Table VI

	Total En.	Binding En.	Electronic En.	Multiplicity
C_2^{-2}	-21.7359	-0.2043	-31.0742	1
	-21.0335	-0.1019	-30.90718	3
B_3^{-2}	-33.0362	-0.7388	-57.6573	1
	-32.9485	-0.6511	-57.5696	3
C_4^{-2}	-44.4197	-1.3560	-92.2475	1
	-44.3773	-1.3141	-93.3566	3
B_5^{-2}	-54.7251	-1.6254	-120.4505	1
	-55.4713	-1.6422	-121.1967	3
C_6^{-2}	-66.6445	-2.0496	-156.7236	1
	-66.6740	-2.0790	-156.7538	3
B_7^{-2}	-77.6563	-2.2955	-194.1540	1
	-77.9026	-2.5419	-194.4004	3
C_8^{-2}	-89.0680	-2.9415	-233.5765	1
	-89.1094	-2.9829	-233.6179	3

Table VII

Calculated Charge Distribution

Compound	Atom	Electron Population	(Charge)
S_2^{-2} a	S_1, S_2	7.0000	-1.0000
S_3^{-2} a	S_1	6.7971	-0.7971
	S_2	6.4068	-0.4068
	S_3	6.7961	-0.7961
S_4^{-2} a	S_1	6.7728	-0.7728
	S_2	6.2778	-0.2778
	S_3	6.2780	-0.2780
	S_4	6.7214	-0.7214
S_5^{-2}	S_1	6.6367	-0.6367
	S_2	6.2704	-0.2704
	S_3	6.1783	-0.1783
	S_4	6.2813	-0.2813
	S_5	6.6333	-0.6333
S_6^{-2}	S_1	6.5490	-0.5490
	S_2	6.1814	-0.1814
	S_3	6.2696	-0.2696
	S_4	6.2696	-0.2696
	S_5	6.1814	-0.1814
	S_6	6.5490	-0.5490
S_7^{-2}	S_1	6.5155	-0.5155

Table VII Continued

Compound	Atom	Electron Population	(Charge)
S_7^{-2}	S_1	6.5155	-0.5155
	S_2	6.1516	-0.1516
	S_3	6.1940	-0.1940
	S_4	6.2843	-0.2843
	S_5	6.2009	-0.2009
	S_6	6.1514	-0.1514
	S_7	6.5024	-0.5024
S_8^{-2}	S_1	6.4876	-0.4876
	S_2	6.1317	-0.1317
	S_3	6.1418	-0.1418
	S_4	6.2388	-0.2388
	S_5	6.2389	-0.2389
	S_6	6.1421	-0.1421
	S_7	6.1317	-0.1317
	S_8	6.4875	-0.4875

a) spin multiplicity = 1

both Garnder and Fraenkel [17, 18] and Pinkus and Piette [19] rules out small diatomic and triatomic sulfur chain aggregates of four or greater atoms with the unpaired electrons localized near each end of the chain should exhibit some anisctropic spin-gain interaction, but this should probably be small and characterized only by their field independent breadths. In conclusion the spectra of liquid sulfur and solid sulfur in CS_2 probably consists of sulfur chains of approximately eight members of more in length in which anisotropic spin-spin interaction is negligible.

Acknowledgement

The author would like to thank Professor John S Lewis for many helpful discussions. This work has been partially supported by NASA Grant NGL-22-009-521.

1. To be published.
2. F. Feher and H. Munzer, Chem. Ber. 96, 1131 (1963).
3. S.D. Thompson et al., J. Chem. Phys. 54, 1367 (1966).
4. K. Spitzer, B. Meyer and M. Gouterman, 1971, paper presented at the Conference on Molecular Structure and Spectroscopy, Columbus, Ohio.
5. J.A. Pople et al., J. Chem. Phys. 43, 5129 (1965).
6. J.A. Pople and G.A. Segal, J. Chem. Phys. 43, 5136 (1965).
7. D.P. Santry and G.A. Segal, J. Chem. Phys. 47, 158 (1967).
8. Quantum Chemistry Program Exchange, Dept. of Chemistry Indiana University, Bloomington, Indiana 47401.
9. F. Feher and B. and M. Baudler, Z. Electronchem. 47, 844 (1941).
10. J. Donohue and V. Schomaker, J. Chem. Phys. 16, 92 (1948).
11. I.M. Dawson et al.,J. Chem. Soc. 322,(1948).
12. B.E. Warren and J.T. Burwell, J. Chem. Phys. 3, 6, (1935).
13. C.S. Lu and J. Donohue, J. Am. Chem. Soc. 66, 818 (1944).
14. C.C. Price and S. Oae, Sulfur Bonding, Ronald Press Co. New York, 1962.
15. G. Herzberg, Molecular Spectra and Molecular Structure I. Spectra of Diatomic Molecules, 502-581, D. Van Nostrand Co., (1953).
16. R. Gaspar, Acta Phys. Acad. Sci. Hung. 7, 289 (1957).

17. D.M. Gardner and G.K. Fraenkel, J. Am. Chem. Soc. 76, 5891 (1954).

18. D.M. Gardner and G.K. Fraenkel, J. Am. Chem. Soc. 78, 3279 (1956).

19. A.G. Pinkus and L.H. Piette, J. Phys. Chem. 63, 2086 (1959).

20. E. Muller et al. Angew. Chem. 5, 6 (1966).

21. W. Duffy Jr., J. Chem. Phys. 36, 490 (1962).

22. H.R. Falle et al. Mol. Phys. 11, 49 (1966).

Appendix No. 5

LCAO-SCF-INDO Calculations on $NH_2NH_2^+$

LCAO-SCF-INDO Calculations on $NH_2NH_2^+$

Ira R. Pines

Planetary Astronomy Laboratory
Department of Earth and Planetary Sciences
Massachusetts Institute of Technology

August 1971

Contribution No. of the Planetary Astronomy Laboratory

Abstract

INDO molecular orbital calculations have been performed upon $NH_2NH_2^+$ in its ground electronic state. Agreement with the planar structure predicted by Reilly and Marquardt [1] from their qualitative molecular orbital diagram has been found, with the odd electron in the $1b_{2g}$ molecular orbital almost completely localized upon the nitrogen $2p_z$ atomic orbitals. Excellent agreement between experimental isotropic hyperfine coupling constants from ESR spectra and results from INDO calculations has also been found.

Introduction

As observed by Reilly and Marquardt [1], the planar structure of $NH_2NH_2^+$, with 13 valence electrons, is an intermediate between the nonplanar hydrazine and the planar ethylene, with 12 valence electrons. This presents a structurally useful application of M.O. theory in a test of whether approximate LCAO-SCF theory predicts the same structure as Extended Huckle Theory (EHT). Since Walsh diagrams[2] and their orbital interpretations as discussed by Allen[3] are products of Huckel Theory which has been used to predict the planar structure of $NH_2NH_2^+$ qualitatively, INDO calculations have been performed upon $NH_2NH_2^+$ at various twist angles χ to determine the most stable configuration. $NH_2NH_2^+$ has also been subjected to ESR studies [1, 4, and 5] and the isotropic hyperfine coupling constant and s orbital spin densities have been calculated, and in this paper shall be compared with INDO results.

Method of Calculation

The calculations have been carried out using the Pople-Beveridge Dobosh, Intermediate Neglect of Differential Overlap (INDO) Method [6]. The molecular wave function employed is of an unrestricted form:

(1) $\Psi = /\psi_1^{\alpha}(1)\alpha(1) \ldots \psi_p^{\alpha}(p)\alpha(p)\psi_1^{\beta}(p+1)\beta(p+1) \ldots \psi_q^{\beta}(N)\beta(N)/$

where there are α p and β q electrons ($p \geq q$). The unrestricted wave function assigns different electronic spins to spatially distinct orbitals. In this paper the unrestricted formalism shall be retained and for convenience the wave function for α electrons shall be only considered. The molecular orbitals are formed from an orthonormal set:

(2) $\psi_i^{\alpha} = \sum_{\mu} C_{\mu_i}^{\alpha} \phi_{\mu}$

for which $C_{\mu_i}^{\alpha}$ are the linear expansion coefficients of ϕ_{μ}, which are composed of Slater Type Orbitals. In the INDO method in comparison with the CNDO (Complete Neglect of Differential Overlap) [7, 8, 9], the one-center atomic exchange integrals are retained. Retaining the one center integrals introduces qualitatively the effect of Hund's Rule, which states that on the same atom, electrons in different orbitals shall have lower repulsion energies if the spins are parallel. The resultant effect is to introduce some spin density into the σ system for π odd electron radicals leading to a non-zero isotropic hyperfine coupling constant.

The F matrices are:

(3) $F_{\mu\mu}^{\alpha} = U_{\mu\mu} + \sum_{\lambda}^{A}[P_{\lambda\lambda}(\mu\mu/\lambda\lambda) - P_{\lambda\lambda}^{\alpha}(\mu\lambda/\mu\lambda)] +$

$+ \sum_{B \neq A} (P_{BB} - Z_B)\gamma_{AB}$ (μ on atom A)

(4) $F^{\alpha}_{\mu\nu} = (2P_{\mu\nu} - P^{\alpha}_{\mu\nu})\ (\mu\nu/\mu\nu) - P^{\alpha}_{\mu\nu}\ (\mu\nu/\nu\nu)$

$(\mu \neq \nu)$ both on atom A

where:

$$P^{\alpha}_{\mu\nu} = \sum_{i}^{p} C_{\mu_i}^{\alpha}\, C^{\alpha}_{\nu_i}$$

$$P_{\mu\nu} = P^{\alpha}_{\mu\nu} + P^{\beta}_{\mu\nu}$$

γ_{AB} is approximated by a Coulomb Integral of the type $(S_A S_A / S_B S_B)$ involving S type orbitals upon A and B [6]. The core integrals $U_{\mu\mu}$ are calculated by subtracting the electron interaction terms from the mean ionization potential I and electron affinity A of appropriate atomic states [6]1. The isotropic hyperfine coupling constant is given by the relation:

(5) $a_N = [\frac{4\pi}{3}\, g\beta\gamma_N\ \ S_z^{-1}/\phi_{sn}(R_n)/^2]\ p^{spin}_{sn\ sn}$

where g is the electronic g factor, β is the Bohr magneton, γ_n is the gyromagnetic ratio for nucleus N, S_z is the spin angular momentum component, $\phi_{sn}(R_n)$ is the valence S orbital wave function at Rn, and p^{spin}_{SnSn} the isotropic hyperfine coupling constant is calculated.

Parameters used in the INDO calculations and the molecular geometry [1] are presented in Table I. The calculations were performed on the M.I.T. IBM 360-65 computer using a program provided by the Quantum Chemistry Program Exchange [11].

Table I

Orbital	Atom	$-\frac{1}{2}(I+A)$*	$-U_{\mu\mu}$*	$\gamma_{\mu\mu}$*
1s	H	7.176	13.601	12.85
2s	N	19.316	90.724	11.05
2p	N	7.275	78.906	11.05

	X(Å)	Y(Å)	Z(Å)
N1	0.000	0.0	0.0
N2	1.33	0.0	0.0
H1	-0.413	0.998	0.0
H2	-0.413	-0.998	0.0
H3	1.712	0.998	0.0
H4	1.712	-0.998	0.0

$R_{N-N} = 1.33\text{Å}$

$R_{N-H} = 1.08\text{Å}$

LH-N-H = 123.5°

*e.V.

Results and Discussion

A. Structure of $NH_2NH_2^+$

Table II shows the calculated total energy, electronic energy, nuclear repulsion energy, binding energy and dipole moment of $NH_2NH_2^+$ for various twist angles χ between the 0° planar and 90° perpendicular configurations. The most stable structure predicted is the planar $NH_2NH_2^+$ with D_{2n} symmetry. This structure is approximately 1.62 eV more stable than the perpendicular configuration.

Table III presents the calculated charge distribution for $NH_2NH_2^+$. The hydrogen atoms carry most of the positive charge with a small positive charge residing on each nitrogen atom. The overall charge distribution in a molecule is reflected by the total dipole moment. The major contributions to the dipole moment are a) the net atomic charge densities and b) the atomic sp polarization resulting from a mixing of s and p orbitals on each atom. The calculated contributions to the total dipole moment are shown in Table IV. The positive dipole moment is defined in the sense of $NH_2 \rightarrow NH_2^+$ in the direction of the molecular axis. The dipole moment decreases as the twist angle is increased from 0 to 90°. This effect is attributable probably to the fact that charge transfer is favored to the nitrogen atoms, by bending from a linear configuration.

B. Eigenvalues

Applying Koopman's theorem [12], the vertical ionization potential of $NH_2NH_2^+$ is calculated to be 0.7982 A.U. ($\sim$21.59 e.V.). The first ionization potential for hydrazine

Table II

$\chi°$	Total Energy (A.U.)	Electronic Energy (A.U.)	Nuclear Repulsion Energy (A.U.)	Binding Energy (A.U.)	Dipole Moment (D)
0°	-25.0251	-51.5238	-26.4986	-1.1238	3.1182
30°	-25.0164	-51.5082	-26.4818	-1.1151	3.1119
45°	-25.0050	-51.4889	-26.4839	-1.1037	3.1010
60°	-24.9884	-51.4656	-26.4772	-1.0871	3.0734
90°	-24.9606	-51.4280	-26.4674	-1.0593	1.5129

Table III

Calculated Charge Distribution

	Atom	Electron Population	(Charge)
$NH_2NH_2^+$	N	4.9727	+0.0273
	N	4.9727	+0.0273
	H	0.7642	+0.2358
	H	0.7642	+0.2358
	H	0.7625	+0.2375
	H	0.7625	+0.2375

Table IV

Dipole Moment

	X(D)	Y(D)	Z(D)
a	3.1384	0.0	0.0
b	-0.0202	0.0	0.0
total	3.1182	0.0	0.0

Dipole Moment = 3.1182 Debyes

($NH_2NH_2 \rightarrow NH_2NH_2^+$) is approximately 9.60 e.v.'s, and although the second ionization potential has not bee published, a value of at least twice the first ionization potential is not unreasonable. The eigenvalues and molecular coefficients for the alpha and beta spin are presented in Table V. The 18_{2g} orbitals for both the alphas and beta spin are localized completely on the nitrogen 2pz orbitals which lends support to Reilly and Marquardt's claim that the odd electron is in the $1b_{2g}$ orbital.

C. Spin Density

Table VI presents the total and spin density matrices. The total density matrix which is just the sum of the alpha and beta electron matrices, and the spin density matrix which is just the difference between the alpha and beta electron matrices, show a large concentration of electron density in the nitrogen $2p_z$ orbitals. In combination with the weakly bonding nature of the $1b_{2g}$ orbital which may be observed from the molecular coefficients and the large electron density in the nitrogen $2p_z$ orbitals, the three electron bond [14] may be attribuatable to a large electron density in the nitrogen $2p_z$ orbitals.

D. E.S.R. Calculations

EIGENVALUES AND EIGENVECTORS FOR ALPHA SPIN

Table V

$NH_2NH_2^+$ (INDO)

EIGENVALUES---		-2.0423 $1a_{1g}$	-1.5251 $1b_{3u}$	-1.3579 $1b_{2u}$	-1.1804 $2a_{1g}$	-1.1454 $1b_{1g}$	-1.0190 $1b_{1u}$	-0.8522 $1b_{2g}$
N	S	0.6182	-0.5255	0.0031	-0.0000	0.0773	-0.0018	0.0000
N	PX	0.1676	0.3309	-0.0002	0.0002	-0.5442	0.0013	0.0000
N	PY	-0.0012	0.0032	0.6081	-0.0000	0.0017	-0.4621	-0.0000
N	PZ	0.0000	0.0000	0.0000	0.7847	0.0003	-0.0000	0.6199
N	S	0.6182	0.5586	-0.0010	-0.0001	0.0716	0.0008	-0.0000
N	PX	-0.2334	0.2273	-0.0030	-0.0003	0.7129	0.0009	0.0000
N	PY	-0.0006	0.0008	0.5334	-0.0000	0.0012	0.5569	0.0000
N	PZ	0.0000	0.0000	0.0000	0.6199	0.0003	0.0000	-0.7847
H	S	0.2078	-0.2632	0.3211	-0.0001	0.1809	-0.3256	0.0000
H	S	0.2093	-0.2674	-0.3199	-0.0001	0.1801	0.3255	0.0000
H	S	0.1849	0.2345	0.2637	-0.0001	0.2449	0.3640	0.0000
H	S	0.1856	0.2341	-0.2661	-0.0001	0.2437	-0.3632	0.0000

EIGENVALUES AND EIGENVECTORS FOR BETA SPIN

Table V

$NH_2NH_2^+$ (INDO)

EIGENVALUES---		-1.9822 $1a_{1g}$	-1.6272 $1b_{3u}$	-1.4003 $1b_{2u}$	-1.2322 $2a_{1g}$	-1.0082 $1b_{1g}$	-0.7235 $1b_{1u}$	-0.2560 $1b_{2g}$
N	S	-0.6401	0.0074	0.0074	0.0055	-0.0000	-0.0000	0.0000
N	PX	-0.2120	-0.0069	-0.0069	0.0010	0.0000	0.0000	0.0000
N	PY	-0.0041	0.7818	0.7818	-0.0747	0.0000	0.0000	0.0000
N	PZ	0.0000	0.0000	0.0000	-0.0000	-0.8358	-0.8358	-0.5491
N	S	-0.5769	-0.0145	-0.0145	-0.0077	-0.0000	-0.0000	-0.0000
N	PX	0.2100	-0.0045	-0.0045	-0.0090	0.0000	0.0000	0.0000
N	PY	-0.0005	0.1448	0.1448	0.7335	-0.0000	-0.0000	0.0000
N	PZ	0.0000	0.0000	0.0000	-0.0000	-0.5491	-0.5491	0.8358
H	S	-0.2133	0.4317	0.4317	-0.0904	0.0000	0.0000	-0.0000
H	S	-0.2089	-0.4229	-0.4229	0.0949	0.0000	0.0000	-0.0000
H	S	-0.1990	0.0255	0.0255	0.4585	-0.0000	-0.0000	0.0000
H	S	-0.1990	-0.0399	-0.0399	-0.4706	-0.0000	-0.0000	0.0000

TOTAL DENSITY MATRIX

Table VI

$NH_2NH_2^+$ (INDO)

		N2s	Px	Py	Pz	N2s	Px	Py	Pz	Hls	Hls	Hls	Hls
N	S	1.0718	0.0229	0.0141	0.0000	0.4619	-0.3428	0.0072	-0.0000	0.4243	0.4100	0.1405	0.1337
N	PX	0.0229	0.4788	-0.0108	0.0000	0.3720	-0.3964	-0.0010	-0.0000	-0.1120	-0.1007	0.0181	0.0178
N	PY	0.0141	-0.0108	1.8113	0.0000	-0.0195	-0.0073	0.2382	0.0000	1.0276	-1.0133	-0.0005	-0.0194
N	PZ	0.0000	0.0000	0.0000	2.3970	-0.0000	0.0000	0.0000	0.9178	-0.0000	-0.0000	0.0000	0.0000
N	S	0.4619	0.3720	-0.0195	-0.0000	1.0325	-0.0873	-0.0095	0.0000	0.1050	0.1255	0.3733	0.3825
N	PX	-0.3428	-0.3964	-0.0073	0.0000	-0.0873	0.6586	-0.0080	-0.0000	-0.0286	-0.0209	0.1381	0.1469
N	PY	0.0072	-0.0010	0.2382	0.0000	-0.0095	-0.0080	1.1820	0.0000	0.0482	-0.0418	0.6898	-0.7028
N	PZ	-0.0000	-0.0000	0.0000	0.9178	0.0000	-0.0000	0.0000	1.6030	-0.0000	-0.0000	-0.0000	-0.0000
H	S	0.4243	-0.1120	1.0276	-0.0000	0.1050	-0.0286	0.0482	-0.0000	0.7807	-0.3914	0.0101	0.1044
H	S	0.4100	-0.1007	-1.0133	-0.0000	0.1255	-0.0209	-0.0418	-0.0000	-0.3914	0.7664	0.1177	0.0177
H	S	0.1405	0.0181	-0.0005	0.0000	0.3733	0.1381	0.6898	-0.0000	0.0101	0.1177	0.6022	-0.2317
H	S	0.1337	0.0178	-0.0194	0.0000	0.3825	0.1469	-0.7028	-0.0000	0.1044	0.0177	-0.2317	0.6156

SPIN DENSITY MATRIX

Table VI

$NH_2NH_2^+$ (INDO)

		N2s	Px	Py	Pz	N2s	Px	Py	Pz	Hls	Hls	Hls	Hls
N	S	0.2519	-0.2484	-0.0133	0.0000	-0.2762	-0.0736	-0.0073	-0.0000	0.1396	0.1538	-0.1210	-0.1138
N	PX	-0.2484	0.3887	0.0091	0.0000	0.1270	-0.3074	0.0013	-0.0000	-0.1904	-0.2011	-0.0665	-0.0668
N	PY	-0.0133	0.0091	-0.6447	0.0000	0.0198	0.0073	-0.1042	-0.0000	-0.3378	0.3218	-0.0133	0.0334
N	PZ	0.0000	0.0000	0.0000	-0.3970	-0.0000	0.0000	-0.0000	-0.9178	0.0000	0.0000	0.0000	0.0000
N	S	-0.2762	0.1270	0.0198	-0.0000	0.3660	0.1546	0.0097	0.0000	-0.1175	-0.1385	0.1523	0.1433
N	PX	-0.0736	-0.3074	0.0073	0.0000	0.1546	0.5702	0.0081	0.0000	0.0673	0.0609	0.2304	0.2214
N	PY	-0.0073	0.0013	-0.1042	-0.0000	0.0097	0.0081	0.0073	-0.0000	-0.0686	0.0628	-0.0024	0.0152
N	PZ	-0.0000	-0.0000	-0.0000	-0.9178	0.0000	0.0000	-0.0000	0.3970	0.0000	0.0000	-0.0000	-0.0000
H	S	0.1396	-0.1904	-0.3378	0.0000	-0.1175	0.0673	-0.0686	0.0000	-0.0722	0.2670	-0.0359	0.0033
H	S	0.1538	-0.2011	0.3218	0.0000	-0.1385	0.0609	0.0628	0.0000	0.2670	-0.0544	-0.0093	-0.0436
H	S	-0.1210	-0.0665	-0.0133	0.0000	0.1523	0.2304	-0.0024	-0.0000	-0.0359	-0.0093	0.1000	0.1247
H	S	-0.1138	-0.0668	0.0334	0.0000	0.1433	0.2214	0.0152	-0.0000	0.0033	-0.0436	0.1247	0.0871

Table VII

Measurement	A_N[a]	A_H[a]	$a_{2s}(N)$	$a_{1s}(H)$
INDO	11.1699	-15.1119	0.0294	0.0280
	10.9874	-14.6263	0.0290	0.0271
ref 1	11.8±1.4	-12.9±0.6	0.013	0.026
ref 4	11.5	-11.0	0.021	
ref 5	11.0	-11.0		

a) Values are in Gauss

A final test of whether the INDO calculations presented in this paper predict a stable structure for $NH_2NH_2^+$ is the comparison with results calculated from ESR spectra. In Table VII are presented the results of the INDO calculations and the comparison with experimental values of the isotropic hyperfine coupling constant and s orbital spin densities. Agreement between INDO and experimental values, especially the nitrogen isotropic hyperfine coupling constant is considered good. There appears to be little correlation between the 2s spin densities calculated by the INDO method and from ESR spectra. This is attributable to the fact that INDO calculations are performed upon an isolated molecule while the ESR data was acquired from $NH_2NH_2^+$ in a crystal field. This effects the nitrogen 2s unpaired spin density by decreasing the motion in the crystal field [15]. The overall comparison between the INDO and ESR results is excellent considering the level of approximation in the INDO method.

Conclusion

The prediction of a planar structure from ESR spectra and INDO calculations are complementary. Each method is able to place the odd electron in the $1b_{2g}$ orbital, which is basically a nitrogen 2pz orbital. The weakly anti-bonding

nature of this orbital and the large concentration of electron density agree with the qualitative M.O. diagram presented by Reilly and Marquardt from their ESR data.

Acknowledgement

The author wishes to thank Dr. J.S. Lewis for his fruitful advice. This work was supported in part by NASA grant NGL-22-009-521.

References

1. Marquardt, C.L., 1970, J. Chem. Phys. 53, 3248.

2 Reilly, M.H. and Marquardt, C.L., 1970, J. Chem. Phys. 53, 3257.

2. Walsh, A.D., 1953, J. Chem. Soc., 2260, 2266, 2296, 2301.

3. Allen, L.C. and Russell, J.D., 1967, J. Chem. Phys. 46, 1029.

4. Brivati, J.A., et al., 1965, J. Chem. Soc. 6504.

5. Edlund, O., et al., 1968, J. Chem. Phys. 49, 749.

6. Pople, J.S., et al., 1967, J. Chem. Phys. 47, 2026.

7. Pople, J.A. et al., 1965, J. Chem. Phys. 43, 5129.

8. Pople, J.A. and Segal, G.A., 1965, J. Chem. Phys. 43, 5136.

9. Santry, D.P. and Segal, G.A., 1967, J. Chem. Phys. 47, 158.

10. Pople, J.A., et al., 1968, J. Am. Chem. Soc., 90, 4201.

11. Quantum Chemistry Program Exchange, Dept. of Chemistry, Indiana University, Bloomington, Ind. 47401.

12. Koopmans, T., 1933, Physica 1, 204.

13. Vilesov, F.I., 1963, Dokl. Akad. Nauk. SSSR 132, 632.

14. Pauling, L., 1960, The Nature of the Chemical Bond, Cornell University Press, 3rd ed., Ithaca, N.Y.

15. Carrington, A. and McLachlan, A.D., 1967, Introduction to Magnetic Resonance, Harper and Row, New York.